

Sept 2009

YITP-09-59

M2-BRANES THEORIES WITHOUT 3+1 DIMENSIONAL PARENTS VIA UN-HIGGSING

Masato Taki

Yukawa Institute for Theoretical Physics, Kyoto University, Kyoto 606-8502, Japan

taki@yukawa.kyoto-u.ac.jp

Abstract

$\mathcal{N} = 2$ quiver Chern-Simons theory has lately attracted attention as the world volume theory of multiple M2 branes on a Calabi-Yau 4-fold. We study the connection between the stringy derivation of M2 brane theories and the forward algorithm which gives the toric Calabi-Yau 4-fold as the moduli space of the quiver theory. Then the existence of the 3+1 dimensional parent, which is the consistent 3+1 dimensional superconformal theory with the same quiver diagram, is crucial for stringy derivation of M2 brane theories. We also investigate the construction of M2 brane theories that do not have 3+1 dimensional parents. The un-Higgsing procedure plays a key role to construct these M2 brane theories. We find some $\mathcal{N} = 2$ quiver Chern-Simons theories which correspond to interesting Calabi-Yau singularities.

1 Introduction

Various studies have been done on the physics of D-branes. An effective theory on the world volume of coincided D-branes has been studied well: open strings attached to these D-branes give the degree of freedom of the world volume theory and we find a supersymmetric gauge theory which describe it. Meanwhile, there has been only a little understanding of the low energy physics of M-branes since little is known about degree of freedom on M-theory branes.

Recently, there have been important progress toward the understanding of the world volume physics of multiple M2 branes. Even the world volume theory of the M2 branes probing the simplest background \mathbb{C}^4 was not known until quite recently. An obstruction to construct the theory was the requirement of the maximal supersymmetry $\mathcal{N} = 8$ in $2 + 1$ dimensions: $\mathcal{N} > 3$ supersymmetry was difficult to realize on $2 + 1$ dimensional field theory Lagrangians. A clue to the solution of the problem is the work of Schwarz[1] where it was pointed out that the introduction of the supersymmetric Chern-Simons term enables us to construct theories with the extended supersymmetry. Inspired by this observation, Bagger-Lambert [2][3] and Gustavsson [4] found a superconformal Chern-Simons theory, which we call the BLG theory, with manifest $\mathcal{N} = 8$ supersymmetry and $SO(8)$ R-symmetry. 3-algebra plays an important role in their Lagrangian description, which is unusual structure from the viewpoint of field theory. However, the action was rewritten in [5] as a $SU(2) \times SU(2)$ Chern-Simons theory instead of the $SO(8)$ gauge group of BLG. This formulation does not require 3-algebra, and therefore quiver Chern-Simons theories attracted attentions. $\mathcal{N} = 4$ quiver Chern-Simons theories of the type were constructed by Gaiotto-Witten [6][7] extending $\mathcal{N} = 2$ theories of [8]. Theories with $\mathcal{N} = 5, 6$ supersymmetry were given by [9].

The moduli space of the BLG theory for a specific choice of its Chern-Simons level is $\text{Sym}^2(\mathbb{R}^8/\mathbb{Z}_2)$ [10][11], and thus it is believed that the BLG theory with the Chern-Simons level describes two M2 branes probing the $\mathbb{R}^8/\mathbb{Z}_2$ singularity. However, its moduli space for a generic Chern-Simons level lacks interpretation as a singularity probed by M2 branes. It is therefore very difficult to construct M2 brane theories for more complicated singularities, such as the toric Calabi-Yau 4-folds. Meanwhile, Aharony, Bergman, Jafferis and Maldacena [12] introduced a superconformal $SU(N) \times SU(N)$ (or $U(N) \times U(N)$) Chern-Simons theory with manifest $\mathcal{N} = 6$ supersymmetry [13]. It is thought that supersymmetry of this theory would be enhanced to $\mathcal{N} = 8$ for $k = 1, 2$. Since the moduli space of the theory for the quantized Chern-Simons levels $(k, -k)$ is $\text{Sym}^N(\mathbb{C}^4/\mathbb{Z}_k)$, this theory is a candidate for the M2 brane theory of $\mathbb{C}^4/\mathbb{Z}_k$ for an arbitrary choice of $(k, -k)$. Moreover, the ABJM formulation is very compatible with the extension to M2 brane theories for more complicated backgrounds.

It is also very interesting to generalize the ABJM theory to theories with less supersymmetry.

The world volume theory of M2 branes on a Calabi-Yau 4-fold $X = C(Y)$, which is a cone over a 7 dimensional Sasaki-Einstein manifolds Y , is believed to be dual to M-theory on the background $AdS_4 \times Y$, which preserves $\mathcal{N} = 2$ supersymmetry. For this reason, $\mathcal{N} = 2$ quiver Chern-Simons theories have been investigated as candidates for the duals of these backgrounds [14][15][16]. It is not so easy to construct a Chern-Simons theory whose moduli space is a Calabi-Yau 4-fold. Then the so-called “brane tiling” (or “dimer model”) method [17][18][19] provides a powerful way to find a large class of $\mathcal{N} = 2$ quiver Chern-Simons theories which are expected to be dual to $AdS_4 \times Y$ [16][20][21]. M-theory crystals [22][23][24] also play a key role to understand these quiver Chern-Simons theories [25]. In general, many quiver Chern-Simons theories are associated with a single Calabi-Yau 4-fold [26][27][28], which is an analogue of the toric duality [29][30][31][32][33] of D3 brane theories. This phenomena would be very important to understand the low energy physics of M2 branes. Therefore we study and derive these toric phases of M2 brane theories by using the dimer model and the stringy derivation of M2 brane theories.

Many quiver Chern-Simons theories have been constructed by using parent superconformal theories in $3 + 1$ dimensions: we construct a quiver Chern-Simons theory by adopting the quiver of the parent. However it was found that every quiver Chern-Simons theory cannot have a parent theory. This is because the constraints of quiver theory in $3 + 1$ dimensions coming from the vanishing β -functions are absent in superconformal quiver Chern-Simons theories. Thus we study quiver Chern-Simons theories without parents in order to survey the “landscape” of M2 brane theories.

In the first half of this article we study the relation between the forward algorithm and stringy derivation of M2 brane theories. The forward algorithm, which is a method to determine the geometry of the moduli space of a quiver gauge theory, for M2 brane theories has been developed in [14][15][16]. The dimer model description of a quiver Chern-Simons theory plays an important role to formulate the effective forward algorithm. The dimer model is a dual graph of a quiver diagram and the Kasteleyn matrix of the dimer gives the toric data of the moduli space [20]. Meanwhile Aganagic [34] found a string theoretical derivation of M2 brane theories, which gives an inverse algorithm. We study therefore the relation between these two algorithms. Then we find that the existence of the $3 + 1$ dimensional parent theory is crucial to relate these two approach.

In the latter half of the paper we introduce the notion of the grandparent theory and we construct many theories without a consistent parent theory. Then the un-Higgsing procedure plays a key role to construct these theories. In this paper we utilize mainly the specific un-Higgsing of “doubling” type for studying quiver Chern-Simons theories without a consistent parent theory. This un-Higgsing method is applied to quiver theories in recent works [35][36].

This paper is organized as follows. In section 2, we give a brief reviews on the quiver Chern-Simons theory, its moduli space, the forward algorithm and a stringy origin of M2 brane theories. A relation between the forward algorithm and the stringy derivation of M2 brane theories is discussed in section 3. In section 4, we introduce the useful idea of the grandparent theory in order to derive phases of a M2 brane theory from the corresponding Calabi-Yau 4-fold. The notion of "un-Higgsing" also plays a key role in this section. Using the idea developed in the previous section, we derive many M2 brane theories by un-Higgsing orbifold grandparents in section 5. In section 6 we derive three phases of $C(Q^{111})$ theory. Conclusions are found in section 7. In appendix A, we discuss the cofactor expansion formula of the permanent.

2 M2-branes Theories on Calabi-Yau Four-fold singularities

In this section, we give a brief review on the world volume theories of M2-branes probing Calabi-Yau four-fold singularities. It is believed that $\mathcal{N} = 2$ superconformal quiver Chern-Simons theories in three dimension realize these theories. Many techniques have been developed in order to obtain a quiver Chern-Simons theory from a corresponding toric Calabi-Yau geometry and vice versa.

2.1 $\mathcal{N} = 2$ quiver Chern-Simons theories and Higgs branch

To begin with, we review on construction of a $\mathcal{N} = 2$ quiver Chern-Simons theory action by using $\mathcal{N} = 2$ superfield in $2 + 1$ dimensions. Details would be found in [13][14] for example. The Lagrangian of $\mathcal{N} = 2$ quiver Chern-Simons theory is

$$\begin{aligned} S_{\text{CS}} &= \sum_{a=1}^G \frac{k_a}{4\pi} \int d^3x \int d^4\theta \int_0^1 dt \text{tr} [V_a \bar{\mathcal{D}}^\alpha (e^{tV_a} \mathcal{D}_\alpha e^{-tV_a})] \\ &= \sum_{a=1}^G \int \frac{k_a}{4\pi} \text{tr} [A_a \wedge dA_a + \frac{2}{3} A_a \wedge A_a \wedge A_a - \bar{\chi}_a \chi_a + 2D_a \sigma_a]. \end{aligned} \quad (2.1)$$

Here G is the number of the gauge group factors $\prod_{a=1}^G U(N_a)$, and V_a is a vector superfield for the a -th gauge group $U(N_a)$. D and σ are auxiliary fields of the multiplets. In this article we study theories with gauge factors of the same rank $N_1 = N_2 = \dots = N$. See [13][14] for more general

cases.

$$\begin{aligned}
S_{\text{matter}} &= - \sum_{X_{ab}} \int d^3x \int d^4\theta \operatorname{tr} X_{ab}^\dagger e^{-V_a} X_{ab} e^{V_a} + \left[i \int d^2\theta W(X_{ab}) + \text{c.c.} \right] \\
&= \sum_{X_{ab}} \int d^3x \operatorname{tr} \left[\mathcal{D}_\mu X_{ab}^\dagger \mathcal{D}^\mu X_{ab} - |\sigma_a X_{ab} - X_{ab} \sigma_b|^2 + D_a X_{ab} X_{ab}^\dagger - D_b X_{ba}^\dagger X_{ba} \right] \\
&\quad - \sum_{i=1}^E \int d^3x \operatorname{tr} \left[F_i F_i^\dagger - \frac{\partial W}{\partial \phi_i} F_i - \frac{\partial W}{\partial \phi_i}^\dagger F_i^\dagger \right] + \text{fermions}. \quad (2.2)
\end{aligned}$$

X_{ab} is a chiral matter superfield which transforms as the bifundamental representation under the gauge factors $U(N_a) \times U(N_b)$. The matter fields are also denoted by Φ_i and $\mathcal{E} = \{\Phi\} = \{X\}$ is the set of the matter fields. The index i runs from 1 to E , where $E = |\mathcal{E}|$ is the number of the matter fields.

Extensive work has been done to study the moduli space of the supersymmetric gauge theories in 4 and 3 dimensions [37][38][39][29][30][33][17][18][40][14][15][16][20][21][41][26][27][28][42][35][43]. An important point is that the Higgs branch of a $\prod U(N)$ gauge theory for branes probing a toric singularity \mathcal{M} is the symmetric product $\operatorname{Sym}^N \mathcal{M}$ of the abelian moduli space. We focus on $U(1)^G$ Chern-Simons theories, since we are now interested in the Calabi-Yau geometry itself \mathcal{M} which a brane probes. Moreover we study moduli spaces at classical level. The reason classical analysis is sufficient to study the geometry is because it is believed that the moduli space does not be modified by quantum corrections under the toric condition. Thus the moduli spaces we study in this article are classical ones of abelian theories.

Let us continue to study the action of a $\mathcal{N} = 2$ quiver Chern-Simons theory for the abelian gauge group $U(1)^G$. The scalar potential of this theory is given by

$$V = \sum_{i=1}^E \left| \frac{\partial W}{\partial \phi_i} \right|^2 - \sum_{a=1}^G \frac{k_a}{2\pi} D_a \sigma_a + \sum_{X_{ab}} |\sigma_a X_{ab} - X_{ab} \sigma_b|^2 - \sum_{X_{ab}} X_{ab}^\dagger X_{ab} (D_a - D_b). \quad (2.3)$$

Here we have integrated out the auxiliary fields F_i . The first term is the F-term potential, and the others come from the D-terms.

The structure of the F-term equations of quiver Chern-Simons theory

$$F_i^\dagger = \frac{\partial W}{\partial \phi_i} = 0 \quad (2.4)$$

is completely the same as that of $\mathcal{N} = 1$ quiver gauge theories. The set of the solutions is referred to as the master space [44]

$$\mathcal{F} = \{\partial_i W(\phi_i) = 0\} \subset \mathbb{C}^E. \quad (2.5)$$

This algebraic variety for our theory gives a toric Calabi-Yau manifold. The perfect matching variables, as we will see, is very useful to solve the F-term equation, and we can construct the master space as a symplectic quotient:

$$\mathcal{F} = \mathbb{C}^c // U(1)^{c-G-2}. \quad (2.6)$$

Turning now to the D-term equations, difference with $3 + 1$ dimensional quiver gauge theories will be clear. We rewrite the third term of the scalar potential as follows:

$$\sum_{X_{ab}} X_{ab}^\dagger X_{ab} (D_a - D_b) = \sum_{a=1}^G D_a \left[\sum_{b=1}^G X_{ab}^\dagger X_{ab} - \sum_{b=1}^G X_{ba} X_{ba}^\dagger \right] = \sum_{a=1}^G D_a \mu_a(X). \quad (2.7)$$

Here we introduce the moment map μ_a for the a -th gauge group:

$$\mu_a(X) \equiv \sum_{b=1}^G X_{ab}^\dagger X_{ab} - \sum_{b=1}^G X_{ba} X_{ba}^\dagger. \quad (2.8)$$

The equation of motion of the auxiliary field D is given by

$$\mu_a(X) = \frac{k_a \sigma_a}{2\pi}. \quad (2.9)$$

We can regard $\zeta_a \equiv k_a \sigma / 2\pi$ as an analogue of the FI parameter of $3 + 1$ dimensional theories. One essential difference is that ζ is not a parameter but a vacuum expectation value (VEV) of the auxiliary field σ_a . The fields D_a are linear in the action, which is different from the case of $3 + 1$ dimensional gauge theories, and they play therefore a role of Lagrange multipliers. We can therefore integrate out the auxiliary field D with this equation (2.9). After integrating out D , the D-term potential becomes

$$V_{\text{D-terms}} = \sum_{X_{ab}} |\sigma_a X_{ab} - X_{ab} \sigma_b|^2. \quad (2.10)$$

Then we obtain the D-term equations

$$X_{ab}(\sigma_a - \sigma_b) = 0. \quad (2.11)$$

In this article we study, following [14], the special branch on which all the VEV's of matter fields satisfy $X_{ab} \neq 0$. We can rewrite this condition using (2.11)

$$\sigma_1 = \cdots = \sigma_G = \sigma \in \mathbb{R}^*. \quad (2.12)$$

This is the so-called Higgs branch which admits the interpretation as the moduli space of an M2 brane on a Calabi-Yau.

Meanwhile let us sum up (2.9) over $a = 1, \dots, G$. Since $\sum \mu_a = 0$ follows from the definition of μ_a , we find

$$\sum_{a=1}^G k_a \sigma_a = 0. \quad (2.13)$$

On the Higgsed branch, this relation implies

$$\sum_{a=1}^G k_a \sigma = 0. \quad (2.14)$$

The necessary condition for the existence of the branch $\sigma \neq 0$ is therefore given by

$$\sum_{a=1}^G k_a = 0. \quad (2.15)$$

We will study such an assignment of the Chern-Simons levels throughout the paper. We also impose the following condition for simplicity:

$$\gcd(\{k_a\}) = 1. \quad (2.16)$$

From these conditions, the overall $U(1)$ is decoupled from the theory. Moreover the "FI-term" $\zeta_a \propto \sigma k_a$ pick out the special $U(1)$ along the direction of the Chern-Simons level vector k . There exist therefore the remaining $U(1)^{G-2}$ in this theory. Thus the moduli space can be computed as the symplectic quotient of the master space:

$$\mathcal{M} = \mathcal{F} // U(1)^{G-2}. \quad (2.17)$$

Here we impose $G - 2$ D-term conditions and gauge symmetry as the symplectic quotient on the solution space of the F-term equations.

2.2 M2 brane theories, dimer models and moduli spaces

The brane tilings, or the dimer models, have been an important tool to study quiver gauge theories. A dimer model of our interest is a bipartite graph on a 2-torus and we shall describe it as a graph consists of black and white nodes and edges on the fundamental domain of the torus. We will see many dimer models of concrete examples in the following sections. This diagram encodes the information on a quiver theory effectively. It is easy to associate a dimer with a quiver diagram: the dimer model corresponding to a quiver is defined as the dual diagram of the periodic quiver diagram as Fig.1. Each edge labelled by i corresponds to a bifundamental matter chiral superfield $\Phi_i \in \mathcal{E}$ of the quiver theory and each face labelled by a is associated with a gauge group $U(1)_a$. This assignment is very natural since the dimer model is the dual graph of the quiver diagram. We can

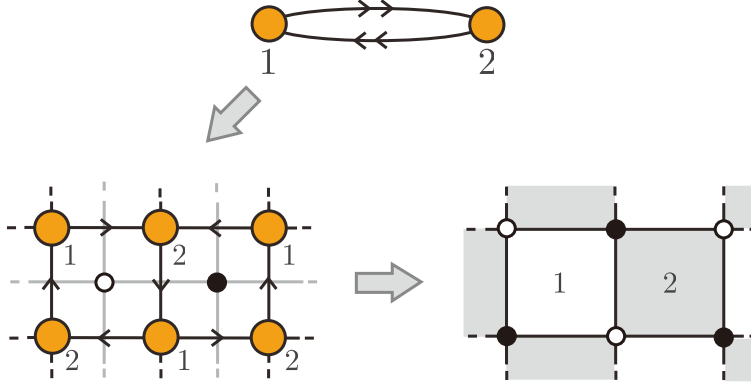


Figure 1: The quiver diagram, the periodic quiver diagram and the dimer model of the ABJM theory.

assign the gauge charges to matters as follows. At first we assign an orientation on the diagram: we define clockwise orientation around white nodes and we define anti-clockwise orientation around black nodes. Let us consider the part of the dimer model Fig.2. The edge i crosses with the

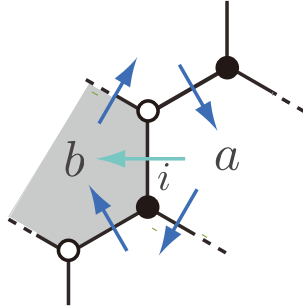


Figure 2: The assignment of the elements $d_{ai} = -d_{bi} = 1$ of the incidence matrix for an edge i .

orientation arrow from the face a to b , and then we define the $U(1)_a$ charge d_{ai} of the matter field Φ_i as follows:

$$d_{ai} = -d_{bi} = 1, \text{ otherwise } d_{ci} = 0. \quad (2.18)$$

In this case Φ_i transforms as the bifundamental representation under $U(1)_a \times U(1)_b$. We also denote Φ_i as X_{ab} . These $U(1)$ charges form the $G \times E$ incidence matrix d . We can rewrite the Chern-Simons levels by using this matrix and integers n_i :

$$k = d \cdot n. \quad (2.19)$$

In this paper we assume that the quiver Chern-Simons theories satisfy the toric condition: each matter field appears in the superpotential precisely twice with opposite sign. Under this

assumption, we can construct the superpotential of the theory from the dimer model:

$$W = \sum_{\circ \in \mathcal{W}} \prod_{i \in \mathcal{E}_\circ} \Phi_i - \sum_{\bullet \in \mathcal{B}} \prod_{i \in \mathcal{E}_\bullet} \Phi_i. \quad (2.20)$$

Here \mathcal{W} and \mathcal{B} are the sets of the white and the black nodes. \mathcal{E}_\circ indicates the set of the edges which are attached to the node \circ . The same is true for the black node \bullet .

The dimer model associated with a quiver theory not only is very useful for the description of the quiver theory, it also gives the effective way to investigate the moduli space of the quiver gauge theory. The forward algorithm is the method to derive the moduli space from the dimer model (or quiver theory). We introduce the Kasteleyn matrix of the dimer model for the purpose. The row of the matrix indices the black nodes of the dimer model and the column indices the white nodes. The (\bullet, \circ) -component of the Kasteleyn matrix is defined by

$$K_{\bullet\circ}(x, y, z) = \sum_{i_{\bullet\circ}} \Phi_{i_{\bullet\circ}} w_{i_{\bullet\circ}}(x, y) z^{n_{i_{\bullet\circ}}}. \quad (2.21)$$

Here $i_{\bullet\circ}$ is an edge which connects the nodes \bullet and \circ . If the edge i crosses the boundary of the fundamental domain, the weight w_i gets the factor x or y (or x^{-1} or y^{-1} according to the orientation). The weight is one if the edge does not cross the boundary.

Let us formulate the fast forward algorithm with the Kasteleyn matrix. The permanent of the Kasteleyn matrix, in particular, is very useful to compute the moduli space:

$$\text{perm} K_{\bullet\circ}(x, y, z) = \sum_{\alpha=1}^c p_\alpha x^{u_\alpha} y^{v_\alpha} z^{q_\alpha} \quad (2.22)$$

See Appendix.A for the definition of perm . The point is that $\text{perm} K$ gives the points $(u_\alpha, v_\alpha, q_\alpha)$ of the toric diagram of the moduli space. We refer to the monomial p_α of the fundamental fields Φ_i as the perfect matchings.

The perfect matching matrix P is also an important object in the forward algorithm. This $E \times c$ matrix is defined by

$$\begin{aligned} P_{i\alpha} &= 1 \text{ if } \Phi_i \in p_\alpha, \\ P_{i\alpha} &= 0 \text{ otherwise.} \end{aligned}$$

The kernel of the matrix $Q_F \equiv \ker P$ gives the charge matrix of the perfect matchings, and therefore we obtain the GLSM description of the Master space:

$$\mathcal{F} = \mathbb{C}^c / Q_F. \quad (2.23)$$

Next we impose the D-term conditions on the space. Let us recall that the incidence matrix d encodes the $U(1)$ charges and the perfect matching matrix transform the matter fields into the

perfect matchings. Thus we can compute the $U(1)$ charges \tilde{Q} of the perfect matchings:

$$d = \tilde{Q} \cdot P^t. \quad (2.24)$$

Only the $U(1)^{G-2}$ symmetry which is orthogonal to 1 and k direction appears in the D-term charge matrix since the two linear combinations of $U(1)$'s for weights 1 and k are decoupled from the theory. The D-term charge is therefore given by

$$Q_D = \ker C \cdot \tilde{Q}, \quad (2.25)$$

where

$$\begin{aligned} C &= \begin{pmatrix} 1 & 1 & \cdots & 1 \\ k_1 & k_2 & \cdots & 0 \end{pmatrix} \\ &= \begin{pmatrix} 1^t \\ k^t \end{pmatrix}. \end{aligned} \quad (2.26)$$

Using these data, we can construct the moduli space as a symplectic quotient:

$$\mathcal{M} = \mathcal{F} // Q_D = (\mathbb{C}^c // Q_F) // Q_D. \quad (2.27)$$

This means that the integral kernel of the total charge ${}^tQ_t = ({}^tQ_D, {}^tQ_F)$ gives the matrix into which the points of the toric diagram are collected:

$$G = \ker Q_t. \quad (2.28)$$

The equivalence between the Kasteleyn matrix method and the symplectic quotient approach was shown in [27].

2.3 Stringy derivation of M2 brane theories

As we saw the algorithm to derive the moduli space from a quiver Chern-Simons theory, we review method to determine the a quiver Chern-Simons theory associated with M2 branes on a Calabi-Yau by utilizing string theory. This inverse algorithm was developed in [34].

Let us consider M2 branes on the following Calabi-Yau 4-fold \mathcal{M} :

$$\sum_{\alpha=1}^c Q_{l\alpha} |X_\alpha|^2 = r_l, \quad l = 1, 2, \dots, c-4. \quad (2.29)$$

We collect the charge vectors $Q_{l\alpha}$ into the $(c-4) \times c$ matrix Q_t which we defined before. The chiral fields X_α are divided by the $U(1)$ gauge groups

$$X_\alpha \rightarrow e^{i\lambda_l Q_{l\alpha}} X_\alpha. \quad (2.30)$$

We can reconstruct the 4-fold as a fibration over a Calabi-Yau 3-fold by adding new variables $r_0 \in \mathbb{R}$ and $\theta_0 \in \mathbb{R}$. First we introduce an additional charge Q_0 which satisfies

$$\sum_{\alpha} Q_{0\alpha} |X_{\alpha}|^2 = r_0 \quad (2.31)$$

and the toric condition $\sum_{\alpha} Q_{0\alpha} = 0$. We can avoid changing the geometry by dividing the additional gauge symmetry:

$$\begin{aligned} \theta_0 &\rightarrow \theta_0 + \lambda_0, \\ X_{\alpha} &\rightarrow e^{i\lambda_0 Q_{0\alpha}} X_{\alpha}. \end{aligned} \quad (2.32)$$

We define the vector q

$$\sum_{\alpha} Q_{0\alpha} q_{\alpha} = 1, \quad \sum_{\alpha} Q_{l\alpha} q_{\alpha} = 0. \quad (2.33)$$

We represent them in matrix notation as $Q_0 \cdot q = 0$ and $Q_t \cdot q = 1_{(c-4)}$.

By fixing r_0 and θ_0 , we can view the 4-fold as a \mathbb{R} and S^1 fibration over the Calabi-Yau 3-fold. The base is defined by

$$\sum_{\alpha=1}^c Q_{l\alpha} |X_{\alpha}|^2 = r_l, \quad (2.34)$$

$$\sum_{\alpha=1}^c Q_{0\alpha} |X_{\alpha}|^2 = r_0. \quad (2.35)$$

This prescription is the starting point of Aganagic's argument in [34].

Let us compactify M-theory on the circle fibered over the base 3-fold \mathcal{M}_3 . The resulting Type IIA superstring theory on $\mathcal{M}_3 \times \mathbb{R}$ contains D2 branes and RR 2-form fluxes $G_{(2)} = dA_{(2)} = \sum q_{\alpha} \omega_{\alpha}$, which are induced from the non-trivial curvature of the fibration [34].

D2 branes on the singularity \mathcal{M}_3 decay into fractional branes and these fractional branes imply the non-trivial quiver gauge theory on 2+1 dimensional world volume. However we expect that the resulting theory is a Chern-Simons theory since our set-up originates from M2 branes on singularity. The point is that the flux through vanishing cycles induces the Chern-Simons terms. Let us consider the fractional brane which is a wrapped D4 brane on a vanishing cycle Δ_a :

$$\sum_{\alpha} Q_{a\alpha} |X_{\alpha}|^2 = t_a. \quad (2.36)$$

Then the Wess-Zumino term on the world volume implies the Chern-Simons levels corresponding to gauge factor Δ_a as

$$\begin{aligned} k_a &= \int_{\Delta_a} G_{(2)} \\ &= \sum_{\alpha} Q_{a\alpha} q_{\alpha} = Q \cdot q. \end{aligned} \quad (2.37)$$

Here we use

$$\int_{\Delta_a} \omega_\alpha^{(2)} = Q_{a\alpha}, \quad (2.38)$$

for the 2-cycle Δ_a . By assuming that the kinetic terms of the gauge fields vanish at IR, we obtain the quiver Chern-Simons theory on the world volume of D2 (or M2) branes. This is the outline of the stringy derivation which was found in [34].

3 Forward Algorithm and Stringy Construction

3.1 Fractional brane and perfect matchings

Aganagic's construction of Calabi-Yau 3-fold and M2 brane theory

Let us recall the inverse algorithm of Aganagic which we reviewed in the previous section. In the inverse algorithm, we start with a Calabi-Yau 4-fold which a M2 brane probes. First we choose a charge vector Q_0 which satisfies ${}^tQ_0 \cdot 1_G = 0$. By adding these GLSM charges $Q_{0\alpha}$ to the original GLSM charges $Q_{\mu\alpha}$ which define the original Calabi-Yau 4-fold, we obtain a Calabi-Yau 3-fold which serves as a $3 + 1$ dimensional parent. The inverse algorithm in $3 + 1$ dimensions is well understood. In this way we obtain a quiver diagram of the M2 brane theory using this parents. Next we define a $G \times 1$ vector q as a solution of the following constraints:

$${}^tQ_0 \cdot q = 1, \quad {}^tQ_\mu \cdot q = 0. \quad (3.1)$$

In addition, we can get the fractional charge matrix $Q_{a\alpha}$ of Calabi-Yau 3-fold. We can therefore find the Chern-Simons level vector k of the M2 brane theory using these data:

$$k = Q \cdot q. \quad (3.2)$$

Forward algorithm for Calabi-Yau 4-fold

Next let us summarize the forward algorithm. The forward algorithm provides a way to determine the Calabi-Yau geometry of the moduli space from the quiver gauge theory which describes the world volume theory of branes on a toric Calabi-Yau singularity. In the forward algorithm, we start with the dimer model which describes a quiver Chern-Simons theory. Using the prescription which we have reviewed in the previous section, we derive the incidence matrix d and the perfect matching matrix P . The relations

$$d = \tilde{Q} \cdot {}^tP, \quad k = d \cdot n \quad (3.3)$$

imply the charge matrix Q and the integral vector n . These data give the toric diagram of the moduli space.

Forward algorithm and Calabi-Yau 3-fold - Proposal

Having seen the inverse and forward algorithms, we are now able to study the relation between them. Comparing (3.2) and (3.3), we propose the relation between these two approaches:

$$Q = \tilde{Q}, \quad q = {}^tP \cdot n. \quad (3.4)$$

This means that the matrix \tilde{Q} gives fractional brane charges with respect to the perfect matchings. In addition, the integers q_α give the third coordinates of the 3 dimensional toric diagram which would be projected out when we derive the 2 dimensional toric diagram of the parent. In other words, the vector q satisfies $Q_t \cdot q = 0$ as follows:

$$\begin{aligned} Q_F \cdot q &= (Q_F \cdot {}^tP) \cdot n = 0, \\ Q_D \cdot q &= Q_D \cdot {}^tP \cdot n = \text{Ker}(C) \cdot \tilde{Q} \cdot {}^tP \cdot n = \text{Ker}(C) \cdot k = 0. \end{aligned}$$

To show the last equality, we use ${}^tv \cdot k = 0$ for $v \in {}^t\text{Ker}(C)$. Thus q_α gives the third coordinate of the point which corresponds to a perfect matching p_α .

In order to relate the forward algorithm with the above-mentioned inverse algorithm, we also have to represent the charge vector Q_0 in the language of the forward algorithm. The point is that Q_0 corresponds to the $U(1)$ charges of GLSM fields for Calabi-Yau 3-fold which is eliminated from the set of $U(1)$ charges in the original Calabi-Yau 4-fold. Similarly, we pick $G - 2$ baryonic $U(1)$'s from $U(1)^G$ when we compute the mesonic moduli space. It is therefore natural that $U(1)$ defined by Q_0 is precisely one of the two remaining $U(1)$'s. In the forward algorithm, the baryonic $U(1)$'s are projected onto the hyperplane \mathbb{Z}^{G-2} orthogonal to 1_c and k via $Q_D = \text{Ker}(C) \cdot \tilde{Q}$. Hence,

$${}^t\tilde{Q} \cdot 1_c, \quad {}^t\tilde{Q} \cdot k, \quad (3.5)$$

are the charges of the remainder which are translated into the language of the perfect matchings. ${}^t\tilde{Q} \cdot 1_c$ cannot be Q_0 , since this $U(1)$ is already encoded in the charge matrix of F-terms ${}^t\tilde{Q} \cdot 1_c \in \text{Ker}(P) = Q_F$. We can show it by using ${}^td = P \cdot {}^t\tilde{Q}$ and $\sum_a d_{ai} = 0$:

$$P \cdot ({}^t\tilde{Q} \cdot 1_G) = {}^td \cdot 1_c = 0_E. \quad (3.6)$$

Then, ${}^t\tilde{Q} \cdot k$ is the only candidate for the charge Q_0 which specifies the Calabi-Yau 3-fold and the parent. We define the following charge vector for our purpose:

$$\hat{Q}_0 = {}^t\tilde{Q} \cdot k. \quad (3.7)$$

It is not so hard to prove that the sum of the charges is zero ${}^t\hat{Q}_0 \cdot 1_c = 0$ by using ${}^tP \cdot 1_E \propto 1_c$ [27]. We have to investigate the inner product of \hat{Q}_0 and q , since Q_0 must satisfy the first equation of

(3.1). The answer is given by

$${}^t\hat{Q}_0 \cdot q = {}^t k \cdot \tilde{Q} \cdot {}^t P \cdot n = {}^t k \cdot k. \quad (3.8)$$

Thus we find a key property of \hat{Q}_0 :

$${}^t\hat{Q}_0 \cdot q = k^2. \quad (3.9)$$

Meanwhile Q_0 is defined by (3.1). It is therefore natural to define the charge vector Q_0 as follows:

$$Q_0 = \frac{1}{k^2} \hat{Q}_0. \quad (3.10)$$

A problem now arises: the definition of Q_0 would not give a integral vector for generic case. We study this problem by taking simple theories for example. Then we propose that the integral answer $\hat{Q}_0/k^2 \in \mathbb{Z}^c$ involves a M2 brane theory with a consistent parent.

3.2 \mathbb{C}^4 theory

Phase I: ABJM theory \mathcal{C}

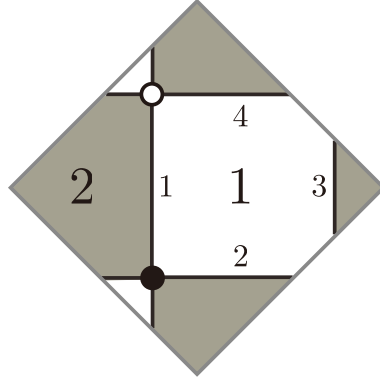


Figure 3: The dimer model of the ABJM theory.

Let us analyze the well-studied M2 brane theory for \mathbb{C}^4 : the ABJM theory. The dimer model and the quiver diagram of the ABJM theory are shown in Fig.3 and Fig.4 respectively. Since this dimer model consists of two square tiles, we shall refer to it as the chessboard model \mathcal{C} following [27]. An important point is that Fig.4 is the same quiver diagram as the well-known Klebanov-Witten theory [50]. Hence the Klebanov-Witten theory is the 3 + 1 dimensional parent for the ABJM theory. We expect that the ABJM theory is related with the conifold, since the Klebanov-Witten theory is a worldvolume theory of D3 branes on the Calabi-Yau 3-fold ¹. The relation has

¹See [48] for a new Seiberg dual description of the Klebanov-Witten theory with $N_c = 2$.

realized in [14][34]: a fibration over the conifold gives the Calabi-Yau 4-fold \mathbb{C}^4 . We review the fact here on the way to the study of the existence of the integer charges Q_0 .

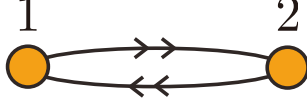


Figure 4: The quiver of the ABJM theory. The Chern-Simons levels are $k_1 = -k_2 = 1$.

The Chern-Simons levels we study here are given by ${}^t k = (1, -1)$. Following the formalism we reviewed in the previous section, we can associate the incident matrix with the dimer model:

$$d = \begin{array}{c|cccc} & \phi_1 & \phi_2 & \phi_3 & \phi_4 \\ \hline 1 & 1 & -1 & 1 & -1 \\ 2 & -1 & 1 & -1 & 1 \end{array} . \quad (3.11)$$

Using the relation $k = d \cdot {}^t n$, we find the integer vector n :

$${}^t n = (0, 0, 1, 0). \quad (3.12)$$

The dimer model Fig.3 also gives the Kasteleyn matrix. Since there are one white node and black node in the dimer, the Kasteleyn matrix is a 1×1 matrix.

$$K = \phi_1 + \phi_2 x + \phi_3 x y z + \phi_4 y. \quad (3.13)$$

Thus the perfect matchings are given by

$$p_1 = X_{12}^1 = \Phi_1, \quad p_2 = X_{12}^2 = \Phi_3, \quad p_3 = X_{21}^2 = \Phi_4, \quad p_4 = X_{21}^1 = \Phi_2. \quad (3.14)$$

There exists therefore a one to one correspondence between matter fields and perfect matchings. The perfect matching matrix is given by

$$P = \begin{pmatrix} 1 & 0 & 0 & 0 \\ 0 & 0 & 0 & 1 \\ 0 & 1 & 0 & 0 \\ 0 & 0 & 1 & 0 \end{pmatrix}. \quad (3.15)$$

The relation $d = \tilde{Q} \cdot {}^t P$ implies the charge matrix of the model:

$$\tilde{Q} = \begin{pmatrix} 1 & 1 & -1 & -1 \\ -1 & -1 & 1 & 1 \end{pmatrix}. \quad (3.16)$$

Then $\hat{Q}_0 = {}^t\tilde{Q} \cdot k$ and ${}^tq = {}^tn \cdot P$ gives

$$\begin{aligned} {}^t\hat{Q}_0 &= (2, 2, -2, -2), \\ {}^tq &= (0, 1, 0, 0). \end{aligned}$$

Hence we find that the relation ${}^t\hat{Q}_0 \cdot q = 2 = k^2$ holds as expeted. These result means that we can find an integer charge vector

$$\begin{aligned} {}^tQ_0 &= \frac{1}{k^2} {}^t\hat{Q}_0 \\ &= (1, 1, -1, -1) \in \mathbb{Z}^4, \end{aligned} \tag{3.17}$$

which satisfies ${}^tQ_0 \cdot q = 1$. Notice that the $U(1)$ charge vector for GLSM fields is precisely the charges for conifold. In other word, the $U(1)$ quotient of Calabi-Yau 4-fold \mathbb{C}^4 implies the conifold $\mathbb{C}^4//U(1)_{Q_0} = \mathcal{C}$ which gives the quiver diagram of ABJM theory as a 3+1 dimensional parent. We propose that the existence of the integer charges such as (3.17) for the ABJM theory is a peculiar feature of the M2 brane theories which have consistent 3 + 1 dimensional parent theories. As we will see in the following examples, M2 brane theories without consistent parents do not implies the integer charges.

Phase II: dual ABJM theory $\mathcal{D}_1\mathcal{H}_1$

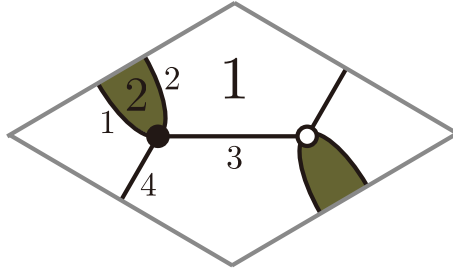


Figure 5: The dimer model of the dual ABJM theory.

It was found in [20] that a quiver Chern-Simons theory which has no cocsistent parents also describes the world volume theory of M2 branes on \mathbb{C}^4 . The dimer model of this theory is drawn in Fig.5. This model is called the one double-bonded one-hexagon model $\mathcal{D}_1\mathcal{H}_1$ [27] since the dimer model consists of tiles in the shape of a hexagon with a double bond. The quiver diagram is shown in Fig.6. The Chern-Simons levels are given by ${}^tk = (1, -1)$. The incidence matrix of the dimer

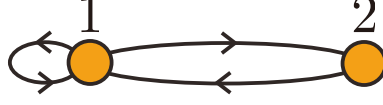


Figure 6: The quiver of the dual ABJM theory. The Chern-Simons levels are $k_1 = -k_2 = 1$.

graph is

$$d = \begin{array}{c|cccc} & \phi_1 & \phi_2 & \phi_3 & \phi_4 \\ \hline 1 & -1 & 1 & d_{13} & d_{14} \\ 2 & 1 & -1 & 0 & 0 \end{array} . \quad (3.18)$$

Here there exists an ambiguity of a choice of components d_{13} and d_{14} . Though we can choose them zero by following [27], we leave them ambiguous. Then we find the integer vector n which satisfy $k = {}^t d \cdot n$:

$${}^t n = (0, 0, 1, 0). \quad (3.19)$$

The perfect matching matrix is

$$P = \begin{pmatrix} 0 & 0 & 1 & 0 \\ 1 & 0 & 0 & 0 \\ 0 & 0 & 0 & 1 \\ 0 & 1 & 0 & 0 \end{pmatrix}, \quad (3.20)$$

where we use the 1×1 Kasteleyn matrix $K = \phi_1 x^{-1} + \phi_2 x^{-1} z + \phi_3 + \phi_4 y$.

We can find an integral solution of the equation $d = {}^t \tilde{Q} \cdot P$:

$$\tilde{Q} = \begin{pmatrix} 1 & d_{14} & -1 & d_{13} \\ -1 & 0 & 1 & 0 \end{pmatrix}. \quad (3.21)$$

Then we obtain

$$\begin{aligned} {}^t \hat{Q}_0 &= {}^t k \cdot \tilde{Q} = (2, d_{14}, -2, d_{13}), \\ {}^t q &= {}^t n \cdot n = (1, 0, 0, 0). \end{aligned}$$

They satisfy ${}^t q \cdot \hat{Q}_0 = 2 = k^2$ as expected.

An important point is that for generic d_{13} and d_{14} the relation

$$Q_0 = \frac{1}{k^2} \hat{Q}_0 \quad (3.22)$$

involves a fractional charge vector Q_0 . With the above-mentioned choice $d_{13} = d_{14} = 0$, Q_0 would be a integer charge vector. Notice that not every M2 brane theory without a parent implies the

integral Q_0 . Therefore the dual ABJM model $\mathcal{D}_1\mathcal{H}_1$ is a peculiar example in that it does not have a consistent parent but gives a integral Q_0 under specific conditions. Below, we investigate some phases without consistent parents which give non-integral charges Q_0 .

3.3 $\mathbb{C} \times \mathcal{C}$ theory

Next let us discuss the phases of the $\mathbb{C} \times \mathcal{C}$ theory which was obtained in [27].

Phase I: The $\mathcal{D}_1\mathcal{C}$ model

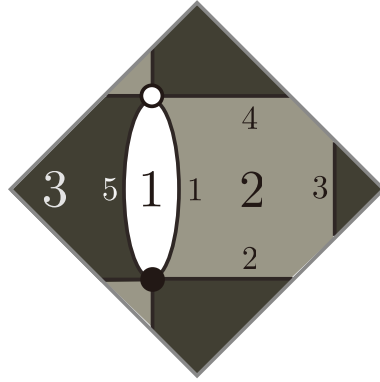


Figure 7: The dimer model of the Phase I of the $\mathbb{C} \times \mathcal{C}$ theory $\mathcal{D}_1\mathcal{C}$.

The dimer model of the Phase I of $\mathbb{C} \times \mathcal{C}$ theory is shown in Fig.7. It is called the one double-bonded chessboard model $\mathcal{D}_1\mathcal{C}$ [27]. The quiver diagram corresponding to the dimer is given in Fig.8. The Chern-Simons levels we study here are ${}^t k = (-1, 1, 0)$. This theory also does not have a

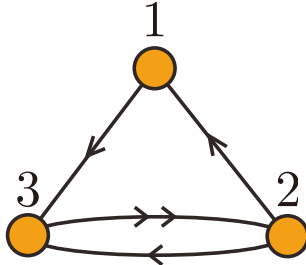


Figure 8: The quiver of the Phase II of the $\mathbb{C} \times \mathcal{C}$ theory. The Chern-Simons levels are ${}^t k = (-1, 1, 0)$.

$3+1$ dimensional parent, since the node 1 of the quiver has $N_f = N_c$ flavors. The incidence matrix

of the model is given by

$$d = \begin{array}{c|ccccc} & \phi_1 & \phi_2 & \phi_3 & \phi_4 & \phi_5 \\ \hline 1 & -1 & 0 & 0 & 0 & 1 \\ 2 & 1 & -1 & 1 & -1 & 0 \\ 3 & 0 & 1 & -1 & 1 & -1 \end{array}. \quad (3.23)$$

Thus we can choose the vector n as

$${}^t n = (1, 0, 0, 0, 0). \quad (3.24)$$

The Kasteleyn matrix of the model is also 1×1 :

$$K = \phi_1 + \phi_2 x + \phi_3 xyz + \phi_4 y + \phi_5. \quad (3.25)$$

The perfect matching matrix is therefore given by

$$P = \begin{pmatrix} 0 & 0 & 1 & 0 & 0 \\ 1 & 0 & 0 & 0 & 0 \\ 0 & 0 & 0 & 1 & 0 \\ 0 & 1 & 0 & 0 & 0 \\ 0 & 0 & 0 & 0 & 1 \end{pmatrix}. \quad (3.26)$$

It is easy to solve the equation $d = \tilde{Q} \cdot {}^t P$ for this matrix P . We find the following integral solution:

$$\tilde{Q} = \begin{pmatrix} 0 & 0 & -1 & 0 & 1 \\ -1 & -1 & 1 & 1 & 0 \\ 1 & 1 & 0 & -1 & -1 \end{pmatrix}. \quad (3.27)$$

We are now able to compute \hat{Q}_0 and q using these data.

$$\begin{aligned} {}^t \hat{Q}_0 &= {}^t k \cdot \tilde{Q} = (-1, -1, 2, 1, -1), \\ {}^t q &= {}^t n \cdot n = (0, 0, 1, 0, 0). \end{aligned}$$

They satisfy ${}^t q \cdot \hat{Q}_0 = 2 = k^2$ as expected. We find that the charge vector Q_0 , which is defined by $Q_0 = \frac{1}{k^2} \hat{Q}_0$, is not integral, which might be a sign of inconsistency of the dimer model in the viewpoint of $3+1$ dimensional gauge theory. Notice that the inconsistency does not give us trouble since we study $2+1$ dimensional Chern-Simons theory.

Phase II: The \mathcal{H}_2 model

The dimer model of the Phase II of $\mathbb{C} \times \mathcal{C}$ theory, which is called the two hexagon model \mathcal{H}_2 [27], is shown in Fig.9. The quiver diagram corresponding to the dimer is given in Fig.10. The

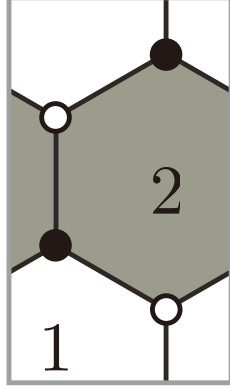


Figure 9: The dimer model of the Phase I of the $\mathbb{C} \times \mathcal{C}$ theory \mathcal{H}_2 .

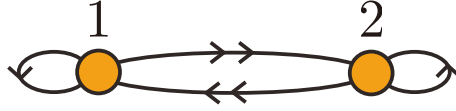


Figure 10: The quiver of the Phase II of the $\mathbb{C} \times \mathcal{C}$ theory. The Chern-Simons levels are ${}^t k = (-1, 1)$.

Chern-Simons levels for the phase are ${}^t k = (1, -1)$. The incidence matrix of the dimer model is given by

$$d = \begin{array}{c|cccccc} & \phi_1 & \phi_2 & \phi_3 & \phi_4 & \phi_5 & \phi_6 \\ \hline 1 & d_{11} & -1 & 1 & 1 & -1 & 0 \\ 2 & 0 & 1 & -1 & -1 & 1 & d_{25} \end{array} . \quad (3.28)$$

Thus we can choose the vector n as

$${}^t n = (0, 0, 1, 0, 0, 0). \quad (3.29)$$

The Kasteleyn matrix of the model is 2×2 , and the permanent of the perfect matching matrix is [27]

$$P = \begin{pmatrix} 0 & 0 & 0 & 0 & 1 \\ 0 & 1 & 0 & 1 & 0 \\ 1 & 0 & 1 & 0 & 0 \\ 1 & 0 & 0 & 1 & 0 \\ 0 & 1 & 1 & 0 & 1 \\ 0 & 0 & 0 & 0 & 1 \end{pmatrix} . \quad (3.30)$$

Then we can solve the equation $d = \tilde{Q} \cdot {}^t P$ as follows:

$$\tilde{Q} = \begin{pmatrix} \tilde{Q}_1 & \tilde{Q}_1 - 2 & 1 - \tilde{Q}_1 & 1 - \tilde{Q}_1 & 0 \\ \tilde{Q}_2 & \tilde{Q}_2 + 2 & -1 - \tilde{Q}_2 & -1 - \tilde{Q}_2 & 0 \end{pmatrix} . \quad (3.31)$$

Here we choose $d_{11} = d_{26} = 0$. Let us compute Q_0 and q using these data.

$$\begin{aligned} {}^t\hat{Q}_0 &= {}^tk \cdot \tilde{Q} = (\tilde{Q}_1 - \tilde{Q}_2, \tilde{Q}_1 - \tilde{Q}_2 - 4, 2 - \tilde{Q}_1 + \tilde{Q}_2, 2 - \tilde{Q}_1 + \tilde{Q}_2, 0), \\ {}^tq &= {}^tn \cdot n = (1, 0, 0, 1, 0, 0). \end{aligned}$$

They satisfy

$$\begin{aligned} {}^tq \cdot \hat{Q}_0 &= (\tilde{Q}_1 - \tilde{Q}_2) + (2 - \tilde{Q}_1 + \tilde{Q}_2) \\ &= 2 = k^2. \end{aligned} \tag{3.32}$$

It is now easy to see that the charge vector

$$Q_0 = \frac{1}{k^2} \hat{Q}_0 \tag{3.33}$$

is not integral for generic \tilde{Q}_1 and \tilde{Q}_2 . However we find a integral Q_0 for a specific choice of $\tilde{Q}_{1,2}$. When substituting $\tilde{Q}_1 = -\tilde{Q}_2 = 1$, for instance, we find

$${}^tQ_0 = (1, -1, 0, 0, 0). \tag{3.34}$$

In this way this theory, which has a consistent $3 + 1$ dimensional parent, implies a integral charge Q_0 .

Phase III: The $\mathcal{D}_2\mathcal{H}_1$ model

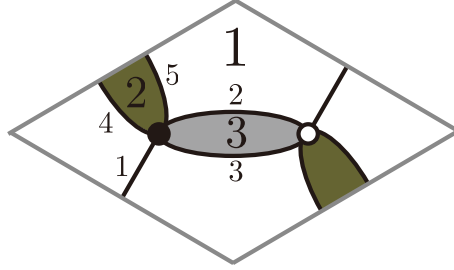


Figure 11: The dimer model of the Phase III of the $\mathbb{C} \times \mathbb{C}$ theory $\mathcal{D}_2\mathcal{H}_1$.

The dimer model of the Phase III of $\mathbb{C} \times \mathbb{C}$ theory is shown in Fig.11. We refer to it as the two double-bonded one-hexagon model $\mathcal{D}_2\mathcal{H}_1$ [27]. The quiver diagram corresponding to the dimer is given in Fig.12. The Chern-Simons levels in this phase are given by ${}^tk = (0, 1, -1)$. The incidence matrix of the dimer model is given by

$$d = \begin{array}{c|ccccc} & \phi_1 & \phi_2 & \phi_3 & \phi_4 & \phi_5 \\ \hline 1 & d_{11} & 1 & -1 & 1 & -1 \\ 2 & 0 & 0 & 0 & -1 & 1 \\ 3 & 0 & -1 & 1 & 0 & 0 \end{array}. \tag{3.35}$$

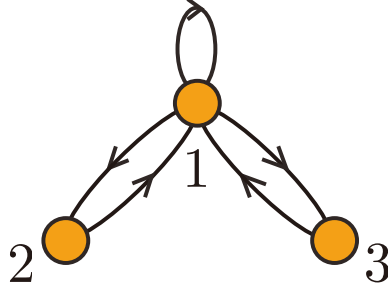


Figure 12: The quiver of the Phase III of the $\mathbb{C} \times \mathcal{C}$ theory. The Chern-Simons levels are ${}^t k = (0, 1, -1)$.

We can solve the equation $k = d \cdot n$, and we find the following integral solution:

$${}^t n = (0, 1, 0, 0, 1). \quad (3.36)$$

The Kasteleyn matrix of the model is the following 1×1 matrix:

$$K = \phi_1 y + \phi_2 z + \phi_3 + \phi_4 x + \phi_5 x. \quad (3.37)$$

Therefore perfect matchings are just the matter fields. The perfect matchi matrix is given by

$$P = \begin{pmatrix} 0 & 0 & 0 & 0 & 1 \\ 0 & 1 & 0 & 0 & 0 \\ 0 & 0 & 0 & 0 & 0 \\ 0 & 0 & 0 & 1 & 0 \\ 0 & 0 & 1 & 0 & 0 \end{pmatrix}. \quad (3.38)$$

We find the following integral solutions of the equation $d = \tilde{Q} \cdot {}^t P$:

$$\tilde{Q} = \begin{pmatrix} 1 & 1 & -1 & -1 & \tilde{Q}_{15} \\ -1 & 0 & 1 & 0 & 0 \\ 0 & -1 & 0 & 1 & 0 \end{pmatrix}. \quad (3.39)$$

Then we find Q_0 and q by using these data:

$$\begin{aligned} {}^t \hat{Q}_0 &= {}^t k \cdot \tilde{Q} = (-1, 1, 1, -1, 0), \\ {}^t q &= {}^t n \cdot n = (0, 1, 1, 0, 0). \end{aligned}$$

They satisfy ${}^t q \cdot \hat{Q}_0 = 2 = k^2$. In this case we obtain the fractional charge vector:

$${}^t Q_0 = \left(0, \frac{1}{2}, \frac{1}{2}, 0, 0 \right). \quad (3.40)$$

This might be a reflection of the fact that a 3 + 1 dimensional parent theory with the quiver Fig.12 gives rise to inconsistency.

3.4 Consistent parents and the inverse algorithm

As we have observed using simple examples, Q_0 would be fractional for a theory without a consistent parent. We expect that a dimer model with a consistent parent theory implies the integral charge vector Q_0 :

$$Q_0 = \frac{1}{k^2} \hat{Q}_0 \in \mathbb{Z}^c. \quad (3.41)$$

It would be interesting to prove the integer property using consistency conditions on dimer models [45][46]. We leave it as an interesting open problem.

For such a integral charge, it is straightforward to define the parent Calabi-Yau 4-fold as a symplectic quotient of the original 4-fold:

$$\mathcal{M}^{\text{qCS}} // U(1)_{Q_0} = \mathcal{M}^{\text{parent}}. \quad (3.42)$$

In this section we have studied relation between the forward and inverse algorithm using dimer model, and we found characteristic feature of a quiver Chern-Simons theory without a consistent parent. It would be desirable to understand the relation from the string theory viewpoint, such as mirror symmetry[47].

4 3 + 1 Dimensional Grandparents, Un-Higgsings, and Theories Without Consistent Parents

In this section, we point out that world volume theories of M2 branes on a toric Calabi-Yau 4-fold are derived from a special class of quiver gauge theories in 3 + 1 dimensions which are associated with the Calabi-Yau 4-fold. We call those 3 + 1 dimensional grandparent theories. Each way to project a toric diagram of a Calabi-Yau 4-fold on a plane gives each grandparent theory. In general, the projected toric diagram has multiplicities which cannot be derived from any 3 + 1 dimensional theories. Therefore we eliminate few points (or multiplicities) from the diagram and define a grandparent whose toric diagram can be realized as a moduli space of a certain 3 + 1 dimensional theory. In the following sections, we work out many examples of the procedure.

In some cases, an M2 brane theory is provided with a consistent 3+1 dimensional parent quiver gauge theory, where the word "consistent" here means that the theory describes a SCFT when flows to IR. This condition constraints the number of flavors for each node of the quiver gauge theory. For an M2 brane theory which has such a parent theory, the 3+1 dimensional parent is just its grandparents by definition.

A grandparent theory leads to an M2 brane theory even if the theory does not have any parent theory. In this case, we add points to the toric diagram of the grandparent theory in order to

recover the projected one of the 4-fold. We employ the so-called un-Higgsing procedure [49] to increase toric points, especially inconsistent un-Higgsing [45] which does not change the area of a toric diagram but increases the number of faces of a dimer model. We refer to the procedure as "un-Higgsing" because with this operation the number of the $U(1)$ gauge symmetry and GLSM fields is increase in the gauged linear sigma model description of the toric 3-fold. As the result, points and multiplicities are added to the toric diagram. In general, a way of projection and un-Higgsing of points is not unique. This ambiguity implies rich landscape of the M2 brane theories. As we will see, a special types of un-Higgsing which is known as "doubling" [35] plays a role in this article.

By turning on Chern-Simons levels of an un-Higgsed theory, we can uplift a 2 dimensional toric diagram and construct a 3 dimensional one. Thus an appropriate choice of Chern-Simons levels leads to the toric diagram of the original Calabi-Yau 4-fold which M2 branes probe. Using these methods, we can construct many quiver Chern-Simons theories which would describe M2 brane theories. The point is that our scheme is applicable to M2 brane theories whether the parents are consistent quiver gauge theories in 4 dimension or not.

We demonstrate the construction of M2 brane theories in some concrete examples using their grandparents. Before discussing new theories, we study two phases proposed in [27] from our viewpoint.

4.1 \mathbb{C}^4 theory

In the previous section, we study two quiver theories and their dimers whose abelian moduli spaces are \mathbb{C}^4 . Using the forward algorithm, we can show that the abelian mesonic moduli spaces of these theories are really \mathbb{C}^4 [27]. At this stage, origin of these theories in the perspective of the Calabi-Yau 4-fold \mathbb{C}^4 is unclear. Therefore, we propose 3 + 1 dimensional grandparents and their un-Higgsings in order to give a detailed explanation of origin of these theories from the Calabi-Yau 4-fold. Our starting point is that we can change the shape of the base of the 3 dimensional toric

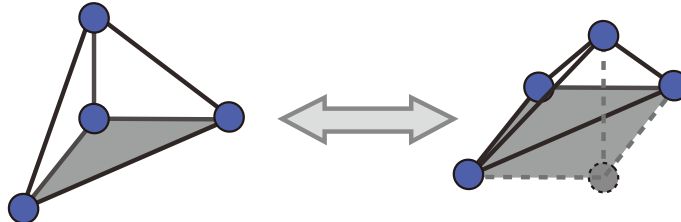


Figure 13: A $SL(3, \mathbb{Z})$ transformation of the toric diagram of \mathbb{C}^4 .

diagram of \mathbb{C}^4 by using $SL(3, \mathbb{Z})$ transformation as Fig.13. One choice of the shape is a right-angled triangle, and the other is a regular square. Then we project the 3 dimensional toric diagram onto the base plane. We regard a projected diagram as a 2 dimensional toric diagram of a Calabi-Yau 3-fold associated with this Calabi-Yau 4-fold. The 2 dimensional toric diagram with the shape of a triangle without internal points is precisely the one of the Calabi-Yau 3-fold \mathbb{C}^3 up to multiplicities of its GLSM fields. The regular square is precisely the toric diagram of the conifold.

It is well known that $\mathcal{N} = 4$ super Yang-Mills theory in $3 + 1$ dimensions is the world-volume theory of D3 branes probing \mathbb{C}^3 . On the one hand, the world-volume theory for the conifold is the well-known Klebanov-Witten theory [50]. We call these two theories the $3 + 1$ dimensional grandparents theories of the M2 brane theories for \mathbb{C}^4 . The dimer models of the grandparents are tilings of hexagons and squares as Fig.14. As we shall see in this section, the two phases of the M2

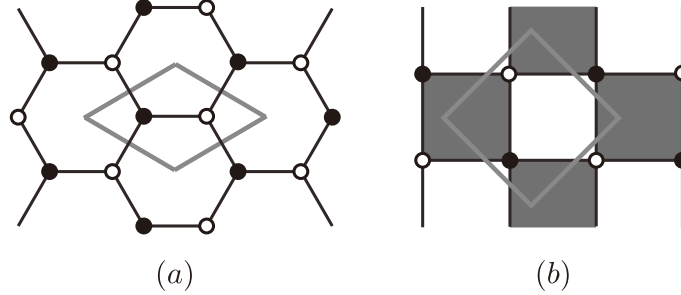


Figure 14: Dimers of the two projected toric diagrams.

brane theory for \mathbb{C}^4 originate from these two grandparents.

Phase I: ABJM theory \mathcal{C}

Let us start with the canonical example known as the ABJM theory. We choose a specific projection of the toric diagram of \mathcal{C} which is shown in the right of Fig.13. This projected toric diagram in 2 dimensions involves the ABJM phase of the \mathbb{C}^4 theory. The grandparent theory emerges from the projection is the conifold theory, since the 2 dimensional diagram is in the shape of a square. Moreover the conifold grandparent is precisely a parent theory of \mathbb{C}^4 theory, since every point in the projected toric diagram has multiplicity 1, which is the same as the conifold theory. The toric diagram and its dimer model are shown in Fig.15. Let us turn to derive the Chern-Simons levels of the \mathbb{C}^4 theory. We shall assign these levels in order that one point of the toric diagram of the parent theory is uplifted and lifted the toric diagram forms a tetrahedron. Recall that the Chern-Simons level vector k is determined by the matrix d and n by using the relation $k = d \cdot n$. Since the matrix d is derived from the dimer of the parent theory, all we have to determine is the choice of the vector

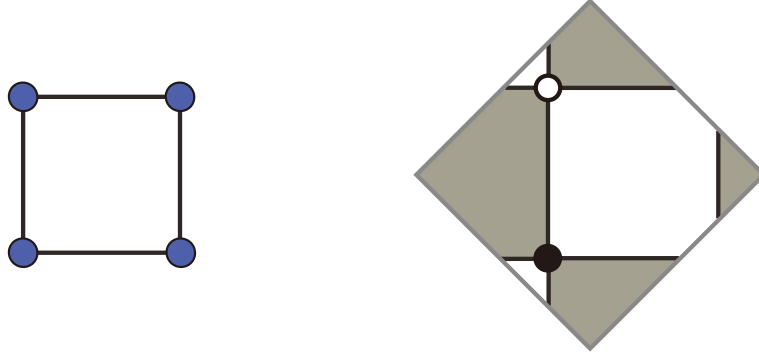


Figure 15: The toric diagram and the dimer model for the conifold (grand)parent.

n .

We follow the convention of the previous section. Let us uplift the point associated with the perfect matching p_1 , in other words we choose n so as to satisfy $q = (1, 0, 0, 0)$. Notice that the coordinates for the third axis are given by $q = {}^tP \cdot n$, where the perfect matching matrix is the same as (3.15). We can solve the equation as follows:

$${}^tn = (1, 0, 0, 0). \quad (4.1)$$

This vector and the incidence matrix (3.11) give k , and therefore we obtain the Chern-Simons levels which make the toric diagram of the moduli space a tetrahedron:

$${}^tk = (1, -1). \quad (4.2)$$

Phase II: dual ABJM theory $\mathcal{D}_1\mathcal{H}_1$

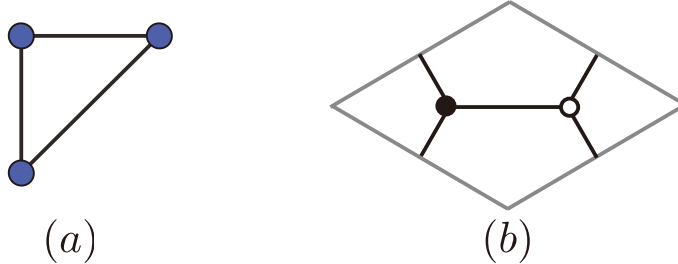


Figure 16: The toric diagram and the dimer model for the \mathbb{C}^3 grandparent.

Let us focus on the grandparent theory associated with \mathbb{C}^3 . The toric diagram and the dimer model for the \mathbb{C}^3 grandparent are shown in Fig.16. Since there exists a point on the top of the tetrahedron, the projection involves a point with multiplicity 2 in the 2 dimensional toric diagram

of the grandparents, which is shown in the left of Fig.13. We have therefore to un-Higgs the grandparent in order to introduce an additional toric point (perfect matchings). One of the simplest choice of un-Higgsing is the so-called "doubling" [35] which introduce a double-bounded edge into the dimer model. The resulting dimer model is denoted in Fig.17. The un-Higgsed model implies

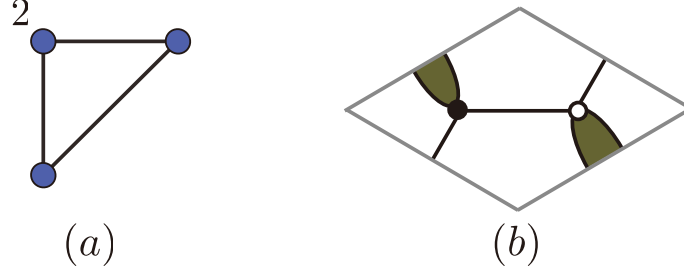


Figure 17: The toric diagram and the dimer model for the \mathbb{C}^3 grandparent.

an additional perfect matching, and the perfect matching matrix becomes the 4×4 identity matrix. Thus one of the points of the 2 dimensional diagram is doubled by un-Higgsing the dimer model. Following the convention of the previous section, the perfect matching matrix of Fig.17 is given by

$$P = \begin{pmatrix} 0 & 0 & 1 & 0 \\ 1 & 0 & 0 & 0 \\ 0 & 0 & 0 & 1 \\ 0 & 1 & 0 & 0 \end{pmatrix}. \quad (4.3)$$

Next we lift one of the doubled perfect matching, p_1 for example, in order to transform the triangle diagram into the tetrahedron. Recall that the third coordinate of a point p_α is given by $q_\alpha = \sum P_{i\alpha} n_i$. We can therefore uplift the perfect matching by turning on the Chern-Simons levels by ${}^t n = (0, 0, 1, 0)$:

$${}^t q = {}^t P \cdot n = (1, 0, 0, 0). \quad (4.4)$$

This choice of n corresponds to the Chern-Simons levels $(k_1, k_2) = {}^t n \cdot d = (1, -1)$. In this way, by turning on an appropriate Chern-Simons levels, the projected toric diagram on a plane is lifted to the 3 dimensional diagram of the Calabi-Yau 4-fold.

5 Un-Higgsings of (3+1) Dimensional Grandparents

In this section, we study the un-Higgsing procedure in concrete examples. We especially focus on grandparent theories whose dimer models are the so-called n hexagons \mathcal{H}_n . The moduli spaces of

the grandparent theories contain abelian orbifolds of \mathbb{C}^3 like $\mathbb{C}^2/\mathbb{Z}_N \times \mathbb{C}$. Then we un-Higgs the grandparents and obtain quiver Chern-Simons theories whose moduli spaces are abelian orbifolds of \mathbb{C}^4 , $C(dP_3) \times \mathbb{C}$ and so forth. See [51][52][53] for orbifold projection of the ABJM theory. In this section we study the orbifold theory by using the dimer model approach. Some of the resulting Chern-Simons theories describes new phases of M2 brane theories.

5.1 $\mathbb{C}^2/\mathbb{Z}_N \times \mathbb{C}$ grandparent

The orbifold $\mathbb{C}^2/\mathbb{Z}_N \times \mathbb{C}$ is one of the well-studied examples of toric Calabi-Yau 3-fold. We un-Higgs these toric Calabi-Yau 3-folds, which play a role of grandparent theories for M2-brane theories. Applying the forward algorithm, we find out that these grandparents implies abelian orbifolds of \mathbb{C}^4 .

Un-Higgsing of $\mathbb{C}^2/\mathbb{Z}_3 \times \mathbb{C}$ grandparent

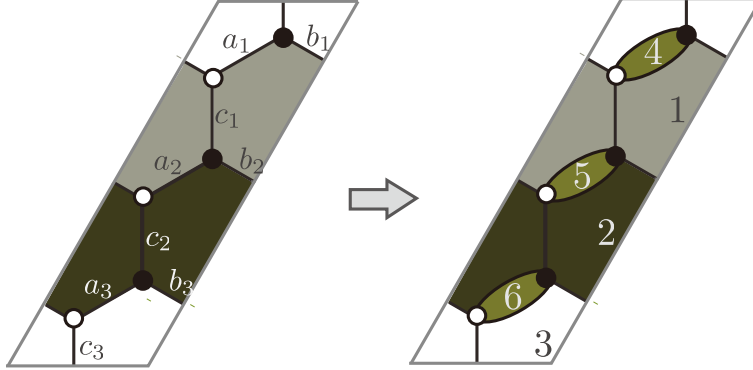


Figure 18: The dimer of $\mathbb{C}^2/\mathbb{Z}_3 \times \mathbb{C}$ grandparent (left) and its un-Higgsing (right).

We first study an un-Higgsed theory for $\mathbb{C}^2/\mathbb{Z}_3 \times \mathbb{C}$ grandparent. As we shall see, we get the M2-brane theory for $\mathbb{C}^3/(\mathbb{Z}_3 \times \mathbb{Z}_3) \times \mathbb{C}$ which was constructed in [21]. We study the un-Higgsing of the dimer of $\mathbb{C}^2/\mathbb{Z}_3 \times \mathbb{C}$ which is illustrated in Fig.18. The Kasteleyn matrix of the grandparent $\mathbb{C}^2/\mathbb{Z}_3 \times \mathbb{C}$ theory is

$$K = \begin{pmatrix} a_1 + b_1x & 0 & c_3y \\ c_1 & a_2 + b_2x & 0 \\ 0 & c_2 & a_3 + b_3x \end{pmatrix}. \quad (5.1)$$

It is easy to compute the permanent of the Kasteleyn matrix:

$$\begin{aligned}
\text{perm}K &= (a_1 + b_1x)(a_2 + b_2x)(a_3 + b_3x) + c_1c_2c_3y \\
&= a_1a_2a_3 + x(b_1a_2a_3 + a_1b_2a_3 + a_1a_2b_3) \\
&\quad + x^2(a_1b_2b_3 + b_1a_2b_3 + b_1b_2a_3) + x^3b_1b_2b_3 + yc_1c_2c_3.
\end{aligned} \tag{5.2}$$

This polynomial consists of 9 monomials. Recall that each monomial coefficient of the term $x^i y^j$

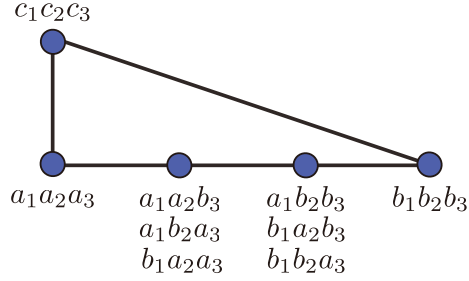


Figure 19: The toric diagram of $\mathbb{C}^2/\mathbb{Z}_3 \times \mathbb{C}$ grandparent and its perfect matchings

corresponds to a point (i, j) , to which is referred as a perfect matching, of the toric diagram. Thus we obtain the toric diagram Fig.19 with total multiplicity 9. Then, we un-Higgs the fields a_n as Fig.20. The effects of the un-Higgsing are captured by the replacement $a_m \rightarrow a_m + a'_m z^{n_{a'_m}}$ in the Kasteleyn matrix. Here we turn on n_i for the un-Higgsed fields a'_m . Then the total number of

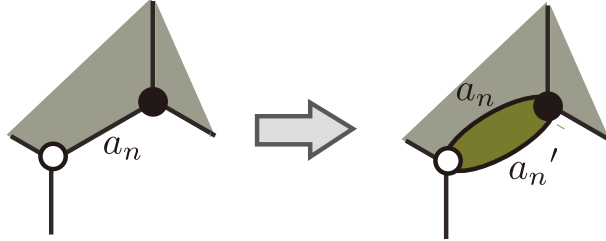


Figure 20: The toric diagram of $\mathbb{C}^2/\mathbb{Z}_3 \times \mathbb{C}$ grandparent and their perfect matchings

perfect matchings becomes $28 = 3^3 + 1$ as Fig.21. Turning on n_i 's, the 2-dimensional toric diagram is lifted to the corresponding 3-dimensional diagram. We can compute the 3-dimensional toric diagram by introducing a third coordinate z into the Kasteleyn matrix. Let us study the following simple case:

$$\begin{aligned}
n_i &= 1 \quad \text{for } i = a'_m, \\
n_i &= 1 \quad \text{otherwise.}
\end{aligned}$$

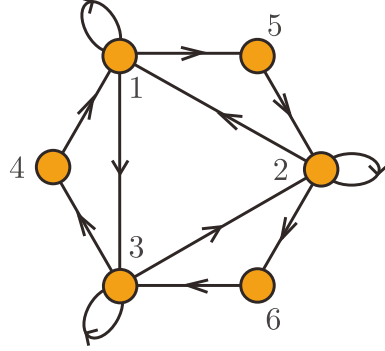


Figure 23: The quiver Chern-Simons theory of M2-branes probing $\mathbb{C}^3/(\mathbb{Z}_3 \times \mathbb{Z}_3) \times \mathbb{C}$. The Chern-Simons level vector is ${}^t k = (1, 1, 1, -1, -1, -1)$.

is given by

$$k_1 = \sum_{i \in \{\text{matters}\}} d_{1i} n_i = d_{1a'1} n_{a'1} = 1. \quad (5.4)$$

Thus we obtain the choice of the Chern-Simons level vector of our interest:

$${}^t k = (1, 1, 1, -1, -1, -1). \quad (5.5)$$

Then we get the quiver Chern-Simons theory whose abelian moduli space is $\mathbb{C}^3/(\mathbb{Z}_3 \times \mathbb{Z}_3) \times \mathbb{C}$. Therefore this theory is the world volume theory of the M2-branes probing the toric singularity $\mathbb{C}^3/(\mathbb{Z}_3 \times \mathbb{Z}_3) \times \mathbb{C}$. Fig.23 is the quiver diagram of the $\mathbb{C}^3/(\mathbb{Z}_3 \times \mathbb{Z}_3) \times \mathbb{C}$ theory. This is precisely the theory which was proposed in [21]. We have re-derived it by using the un-Higgsing approach.

In the rest of this section we apply the un-Higgsing method for several grandparent theories in order to realize that this approach provides an effective method to produce M2-brane theories with and without (3+1)-dimensional parents. Then we find out some new quiver Chern-Simons theories which describe the world volume theories of M2-branes.

Un-Higgsing of $\mathbb{C}^2/\mathbb{Z}_N \times \mathbb{C}$ grandparent

Having obtained $\mathbb{C}^3/(\mathbb{Z}_3 \times \mathbb{Z}_3) \times \mathbb{C}$ theory by un-Higgsing $\mathbb{C}^2/\mathbb{Z}_3 \times \mathbb{C}$, we now generalize the analysis for the grandparent $\mathbb{C}^2/\mathbb{Z}_N \times \mathbb{C}$. The resulting theory describes the theory for the M2-brane probing $\mathbb{C}^3/(\mathbb{Z}_N \times \mathbb{Z}_N) \times \mathbb{C}$. This result gives a proof of the conjecture of [21] that the quiver theory Fig.27 gives $\mathbb{C}^3/(\mathbb{Z}_N \times \mathbb{Z}_N) \times \mathbb{C}$ theory. As we shall see, the Kasteleyn matrix is an effective tool to prove it.

The dimer model of the quiver gauge theory for D3 branes on the orbifold $\mathbb{C}^2/\mathbb{Z}_N \times \mathbb{C}$ is shown in Fig.24. We repeat the above procedure for $\mathbb{C}^2/\mathbb{Z}_N \times \mathbb{C}$. In general there exist many ways to un-

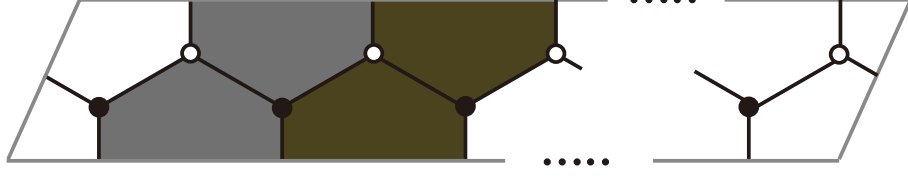


Figure 24: The dimer model for the toric Calabi-Yau 3-fold $\mathbb{C}^2/(\mathbb{Z}_N \times \mathbb{Z}_N) \times \mathbb{C}$.

Higgs the dimer model of a (3+1)-dimensional grandparent theory. However we are now interested in the special type of un-Higgsing, which is a generalization of the case of $\mathbb{C}^2/\mathbb{Z}_3 \times \mathbb{C}$. Thus Fig.25 is the un-Higgsed dimer on which we focus in this article. The superpotential associated with the un-Higgsed dimer model is

$$W = \sum_{n=1}^N \text{tr} (c_n(a'_n a_n b_n - b_{n+1} a'_{n+1} a_{n+1})). \quad (5.6)$$

Here the index $N + 1$ means $N + 1 \equiv 1$. Let us focus on the following choice of the Chern-Simons

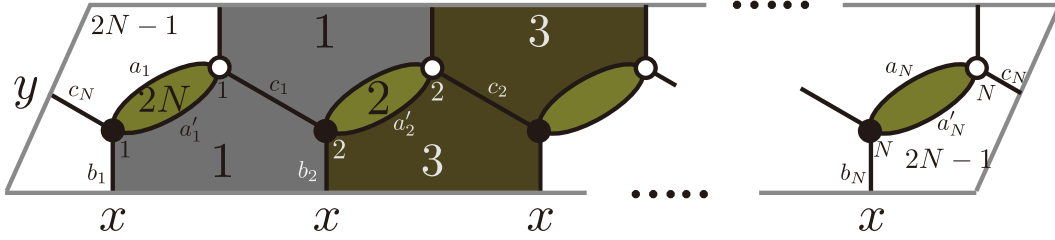


Figure 25: The un-Higgsed dimer model.

levels:

$$n_i = 1 \text{ for } i = a'_m, \quad n_i = 1 \text{ otherwise.} \quad (5.7)$$

The Kasteleyn matrix encodes the toric Calabi-Yau singularity which the mesonic moduli space describes. From the dimer model Fig.24 we easily determine the Kasteleyn matrix for the grandparent

theory:

$$K(a, b, c; x, y) = \begin{pmatrix} a_1 + b_1x & 0 & \cdots & 0 & 0 & c_N y \\ c_1 & a_2 + b_2x & & 0 & 0 & 0 \\ & & \ddots & & & \\ & & & \ddots & & \\ 0 & 0 & & a_{N-2} + b_{N-2} & 0 & 0 \\ 0 & 0 & & c_{N_2} & a_{N-1} + b_{N-1}x & 0 \\ 0 & 0 & \cdots & 0 & c_{N_1} & a_N + b_N x \end{pmatrix}. \quad (5.8)$$

Replacing a_m to $a_m + a'_m z$, we obtain the matrix for the un Higgsed theory Fig.25. The cofactor expansion implies the permanent of (5.8):

$$\text{pern}K(a, b, c; x, y) = \prod_{n=1}^N (a_n + x b_n) + y \prod_{n=1}^N c_n. \quad (5.9)$$

We prove it in Appendix.A. Thus the permanent for the un-Higgsed theory is

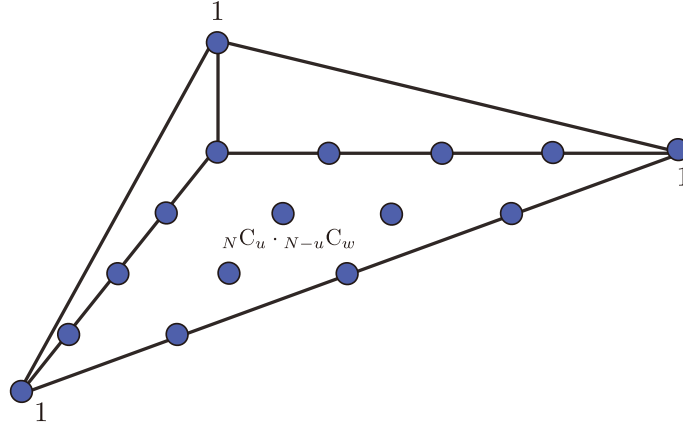


Figure 26: The toric diagram of the moduli space of the un-Higgsed theory. It is precisely the abelian orbifold $\mathbb{C}^3/(\mathbb{Z}_N \times \mathbb{Z}_N) \times \mathbb{C}$.

$$\text{pern}K(a, a', b, c; x, y, z) = \prod_{n=1}^N (a_n + z a'_n + x b_n) + y \prod_{n=1}^N c_n. \quad (5.10)$$

Here we use $n_{a'_n} = 1$. Each monomial of this polynomial is associated with a perfect matching, and a monomial weighted with $x^u y^v z^w$ describes a point (u, v, w) in the toric diagram of the moduli space. Thus the moduli space of the quiver Chern-Simons theory is represented by the toric diagram Fig.26. This is the orbifold $\mathbb{C}^3/(\mathbb{Z}_N \times \mathbb{Z}_N) \times \mathbb{C}$. It is an easy combinatorics to show that

the expansion of the (5.10) implies the multiplicity ${}_N C_u \cdot {}_{N-u} C_w$ for the point $(u, 0, w)$ of the toric diagram. Hence the total multiplicity of the theory is

$$1 + \sum_{u=0}^N \sum_{w=0}^{N-u} {}_N C_u \cdot {}_{N-u} C_w = 1 + 3^N. \quad (5.11)$$

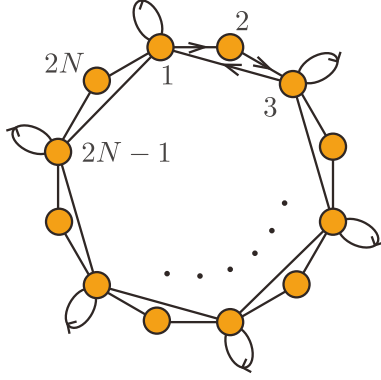


Figure 27: The quiver Chern-Simons theory of M2-branes probing $\mathbb{C}^3/(\mathbb{Z}_N \times \mathbb{Z}_N) \times \mathbb{C}$. The Chern-Simons level vector is ${}^t k = (1, -1, 1, -1, \dots)$.

Let us compute the Chern-Simons levels for this theory. The incidence matrix d is encoded in the dimer model. For instance the nonzero matrix elements for the GLSM field a'_{n+1} are

$$-d_{2na'_{n+1}} = d_{2n+1a'_{n+1}} = 1. \quad (5.12)$$

Thus the assignment (5.7) is identical with the following choice of the Chern-Simons levels:

$${}^t k = {}^t(d \cdot n) = (1, -1, 1, -1, \dots, 1, -1). \quad (5.13)$$

Therefore we obtain the world volume theory of a M2 brane probing $\mathbb{C}^3/(\mathbb{Z}_N \times \mathbb{Z}_N) \times \mathbb{C}$ as Fig.27. This is exactly the theory proposed in [21]. They computed the moduli space only for $N = 3$. Here we prove the proposal for general N by utilizing the power of the Kasteleyn matrix method.

5.2 $\mathbb{C}^3/(\mathbb{Z}_N \times \mathbb{Z}_M)$ grandparent

Next we study the $\mathbb{C}^3/(\mathbb{Z}_N \times \mathbb{Z}_M)$ grandparent theory. The dimer model of the grandparent is shown in Fig.28, and the gauge factors are indexed by (m, n) . We consider the un-Higgsed theory denoted in Fig.29. This un-Higgsing is a simple extension of that in the previous subsection.

We study the quiver Chern-Simons theory with the Chern-Simons levels given by $n_{amn} = 1$. By using the incidence matrix of the un-Higgsed dimer model, this Chern-Simons levels are given by

$$k_{(m,n)} = -1, \quad k_{(m,n)'} = 1. \quad (5.14)$$

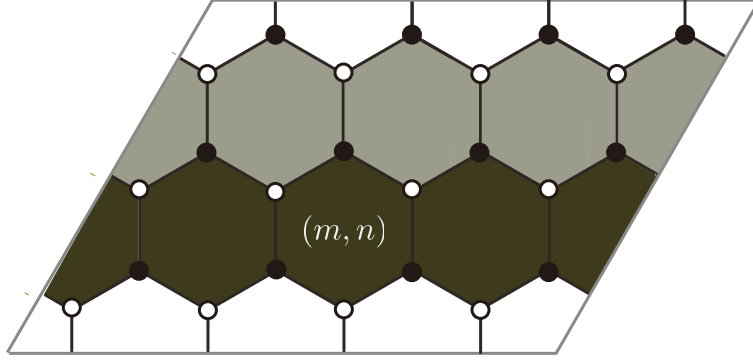


Figure 28: The dimer model of $\mathbb{C}^3/(\mathbb{Z}_N \times \mathbb{Z}_M)$ grandparent theory.

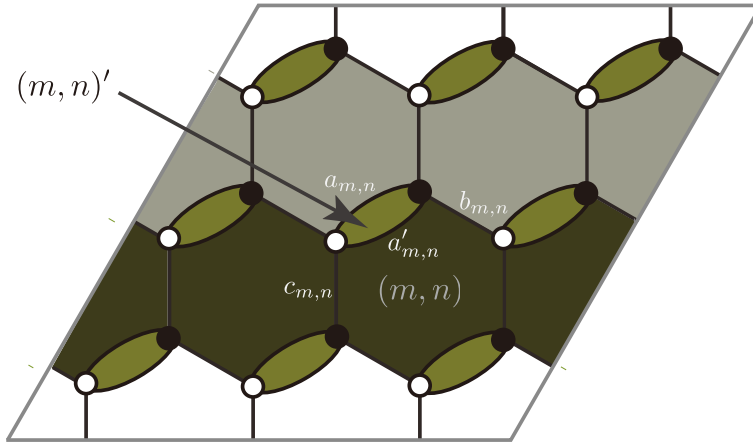


Figure 29: The un-Higgsed dimer model of $\mathbb{C}^3/(\mathbb{Z}_N \times \mathbb{Z}_M)$.

The Kasteleyn matrix of the theory is given by

$$K = \begin{pmatrix} A_1 & B_1 & 0 & \cdots & 0 & 0 \\ 0 & A_2 & B_2 & & 0 & 0 \\ & & \dots\dots\dots & & & \\ 0 & 0 & 0 & & A_{M-1} & B_{M-1} \\ xB_M & 0 & 0 & \cdots & 0 & A_M \end{pmatrix} \quad (5.15)$$

The blocks of the matrix are given by

$$A_m = \begin{pmatrix} a_{m1} + za'_{m1} & 0 & 0 & \cdots & 0 & yc_{mN} \\ c_{m1} & a_{m2} + za'_{m2} & 0 & & 0 & 0 \\ & & \dots\dots\dots & & & \\ 0 & 0 & 0 & \cdots & c_{mN-1} & a_{mN} + za'_{mN} \end{pmatrix} \quad (5.16)$$

and $B_m = \text{diag}(b_{m1}, b_{m2}, \dots, b_{mN})$.

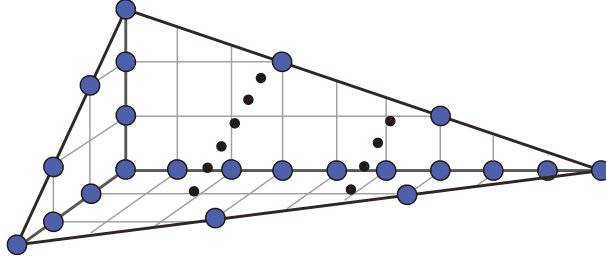


Figure 30: The toric diagram of the moduli space of the un-Higgsed theory. We omit internal points from the figure for simplicity.

Let us analyze the specific example with $M = N = 3$. The following formula, which was given in [17], is useful to compute the toric diagram of the moduli space:

$$\det K = \det(A_1 A_2 A_3) \det(1 - x A_1^{-1} B_1 A_2^{-1} B_2 A_3^{-1} B_3). \quad (5.17)$$

For generic matrix element a , b and c , we can recast it into $\text{perm} K$ by forgetting signs. Thus we obtain the toric diagram Fig.30.

5.3 $(\mathbb{C}^2/\mathbb{Z}_2) \times \mathbb{C}$ grandparent

We shall discuss the grandparent theory corresponding to the orbifold $(\mathbb{C}^2/\mathbb{Z}_2) \times \mathbb{C}$. The dimer model of it is shown in the left of Fig.31. This dimer is called the \mathcal{H}_2 model.

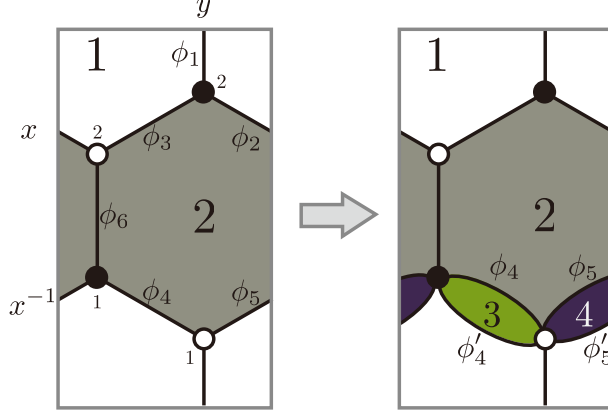


Figure 31: The dimer model for $\mathbb{C}^2/\mathbb{Z}_2 \times \mathbb{C}$ (left) and its un-Higgsing (right).

New phase of $C(dP_3) \times \mathbb{C}$ theory: The $\mathcal{D}_2\mathcal{H}_2$ model

We shall discuss the grandparent theory corresponding to the orbifold $(\mathbb{C}^2/\mathbb{Z}_2) \times \mathbb{C}$. The dimer model of it is shown in the left of Fig.31. This dimer is called the \mathcal{H}_2 model. The Kasteleyn matrix of the dimer model is the following 2×2 matrix:

$$K = \begin{pmatrix} \phi_5 x^{-1} + \phi_4 & \phi_6 \\ \phi_1 y & \phi_2 x + \phi_3 \end{pmatrix}. \quad (5.18)$$

Here the rows and the columns are indexed by the black and white nodes. The permanent of the matrix consists of five terms:

$$\text{perm} K = \phi_2 \phi_5 + \phi_3 \phi_4 + x \phi_2 \phi_4 + x^{-1} \phi_3 \phi_5 + y \phi_1 \phi_6. \quad (5.19)$$

Thus we obtain the perfect matchings matrix:

$$P = \begin{array}{c|ccccc} & p_1 & p_2 & p_3 & p_4 & p_5 \\ \hline \phi_1 & 0 & 0 & 0 & 0 & 1 \\ \phi_2 & 1 & 0 & 1 & 0 & 0 \\ \phi_3 & 0 & 1 & 0 & 1 & 0 \\ \phi_4 & 0 & 1 & 1 & 0 & 0 \\ \phi_5 & 1 & 0 & 0 & 1 & 0 \\ \phi_6 & 0 & 0 & 0 & 0 & 1 \end{array} \quad (5.20)$$

These five perfect matchings form the toric diagram of the moduli space. The diagram is shown in Fig.32. This geometry is precisely the orbifold $\mathbb{C}^2/\mathbb{Z}_2 \times \mathbb{C}$ as expected.

Let us leave the grandparent theory and turn to investigate un-Higgsings of the grandparent theory. For the present, we shall concentrate on an un-Higgsing which adds 2 double bonds.

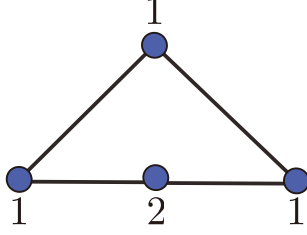


Figure 32: The toric diagram of $\mathbb{C}^2/\mathbb{Z}_2 \times \mathbb{C}$.

The un-Higgsed dimer model we study now is drawn in the right of Fig.31. We shall call this theory the two double-bonded two-hexagon model $\mathcal{D}_2\mathcal{H}_2$. Fig.34 indicates the quiver diagram of the $\mathcal{D}_2\mathcal{H}_2$ model. The superpotential is given by

$$W = \text{tr} (\phi_1(X_{13}X_{32}X_{24}X_{41} - X_{12}X_{21}) - \phi_6(X_{24}X_{41}X_{13}X_{32} - X_{21}X_{12})). \quad (5.21)$$

The doubling procedure on the edges of the grandparent increases the multiplicities of the toric diagram. The additional perfect matchings are

$$\begin{aligned} p'_1 &= \phi_2\phi'_5, & p'_4 &= \phi_3\phi'_5, \\ p'_2 &= \phi_3\phi'_4, & p'_3 &= \phi_2\phi'_4. \end{aligned} \quad (5.22)$$

We can indicate this by plotting these perfect matchings on the xy -plane as Fig.33. We collect them into the perfect matching matrix:

$$P = \begin{array}{c|cccccccccc} & p_1 & p_2 & p_3 & p_4 & p_5 & p'_1 & p'_2 & p'_3 & p'_4 \\ \hline \phi_1 & 0 & 0 & 0 & 0 & 1 & 0 & 0 & 0 & 0 \\ \phi_2 & 1 & 0 & 1 & 0 & 0 & 1 & 0 & 1 & 0 \\ \phi_3 & 0 & 1 & 0 & 1 & 0 & 0 & 1 & 0 & 1 \\ \phi_4 & 0 & 1 & 1 & 0 & 0 & 0 & 0 & 0 & 0 \\ \phi'_4 & 0 & 1 & 1 & 0 & 0 & 0 & 1 & 1 & 0 \\ \phi_5 & 1 & 0 & 0 & 1 & 0 & 0 & 0 & 0 & 0 \\ \phi'_5 & 1 & 0 & 0 & 1 & 0 & 1 & 0 & 0 & 1 \\ \phi_6 & 0 & 0 & 0 & 0 & 1 & 0 & 0 & 0 & 0 \end{array} \quad (5.23)$$

Let us focus on a specific choice of Chern-Simons levels. We choose

$$n_{4'} = -n_{5'} = 1, \quad \text{otherwise } n_i = 0. \quad (5.24)$$

This means that the Chern-Simons levels are given by

$${}^t k = (2, 0, -1, -1). \quad (5.25)$$

Then the perfect matchings p'_1 , p'_2 , p'_3 and p'_4 are lifted up. Their third coordinates, which are given by the formula $q = {}^tP \cdot n$, are

$$q_{1'} = q_{4'} = -1, \quad q_{2'} = q_{3'} = 1. \quad (5.26)$$

Thus the uplifted toric diagram forms $dP_3 \times \mathbb{C}$ as Fig.33.

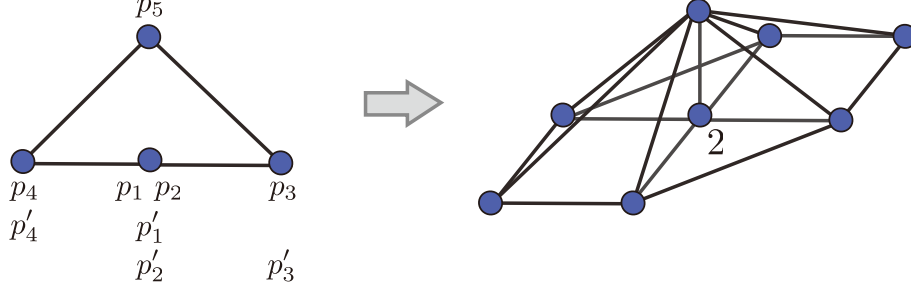


Figure 33: The toric diagram of the moduli space which describes $dP_3 \times \mathbb{C}$ (right) and its projection (left).

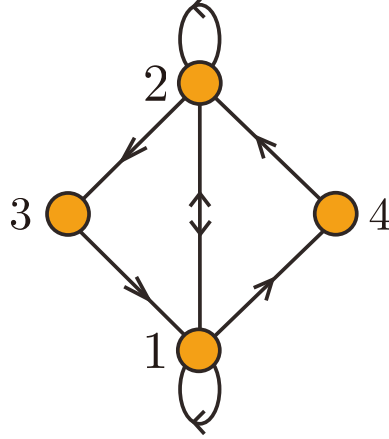


Figure 34: The quiver diagram of a world volume theory of M2 branes on $dP_3 \times \mathbb{C}$. The Chern-Simons levels are ${}^tk = (2, 0, -1, -1)$.

New phase of $\mathbb{C}^2/\mathbb{Z}_2 \times \mathbb{C}^2$ theory: The $\mathcal{D}_1\mathcal{H}_2$ model

Next let us consider the un-Higgsed $\mathbb{C}^2/\mathbb{Z}_2 \times \mathbb{C}^2$ theory Fig.35 of different type. We refer to it as the $\mathcal{D}_1\mathcal{H}_2$ model. The superpotential is given by

$$W = \text{tr} \left(\epsilon_{st} \phi_1 X_{12}^s X_{21}^t + \epsilon_{st} X_{23} X_{32} X_{21}^s X_{12}^t \right). \quad (5.27)$$

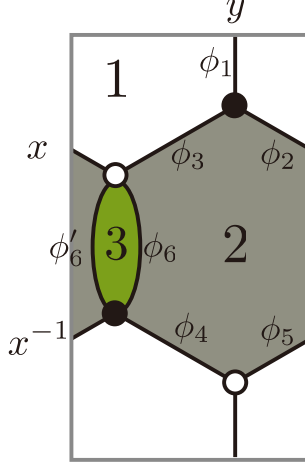


Figure 35: An un-Higgsing of $\mathbb{C}^2/\mathbb{Z}_2 \times \mathbb{C}^2$ theory.

Here X_{12}^s and X_{21}^t transform as the fundamental representation under a global $SU(2)$ symmetry.

The Kasteleyn matrix of the dimer is

$$K = \begin{pmatrix} \phi_5 x^{-1} + \phi_4 & \phi_6 + \phi_6' \\ \phi_1 y & \phi_2 x + \phi_3 \end{pmatrix}. \quad (5.28)$$

Therefore its permanent consists of 6 perfect matchings:

$$\text{perm} K = \phi_3 \phi_4 + \phi_3 \phi_5 + x^{-1} \phi_3 \phi_5 + x \phi_2 \phi_4 + y \phi_1 (\phi_6 + \phi_6'). \quad (5.29)$$

The toric diagram of this model therefore has the same shape of $\mathbb{C}^2/\mathbb{Z}_2 \times \mathbb{C}^2$ theory, however there is an additional perfect matching $p_5' = \phi_1 \phi_6'$ as Fig.36. Let us lift up the point and construct a tetrahedron toric diagram.

Let us turn on $n_{6'} = 1$. This corresponds to the following Chern-Simons levels of the quiver theory Fig.37:

$${}^t k = (0, -1, 1) \quad (5.30)$$

This choice of the Chern-Simons levels lifts the perfect matching p_5' as $q_{p_5'} = P_{6'p_5'} n_{6'} = 1$. Then the toric diagram of the moduli space is given by Fig.36. This is the toric diagram of the abelian orbifold $\mathbb{C}^2/\mathbb{Z}_2 \times \mathbb{C}^2$. Hence we obtain the worldvolume theory of M2 branes which probe $\mathbb{C}^2/\mathbb{Z}_2 \times \mathbb{C}^2$ Fig.37.

5.4 \mathbb{C}^3 grandparent

Finally let us examine a very simple grandparent theory corresponding to \mathbb{C}^3 , where the corresponding dimer is a tiling of hexagons \mathcal{H}_1 . An un-Higgsing operation we will consider introduces a

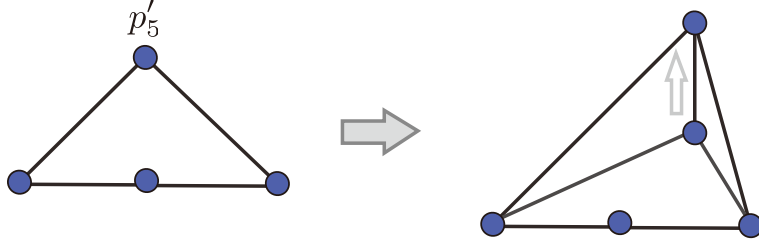


Figure 36: The lift of the toric diagram.

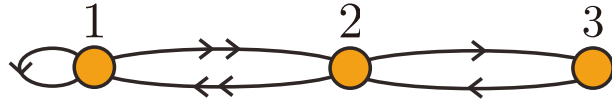


Figure 37: The quiver diagram of $\mathbb{C}^2/\mathbb{Z}_2 \times \mathbb{C}^2$ theory. The Chern-Simons levels are given by ${}^t k = (0, -1, 1)$.

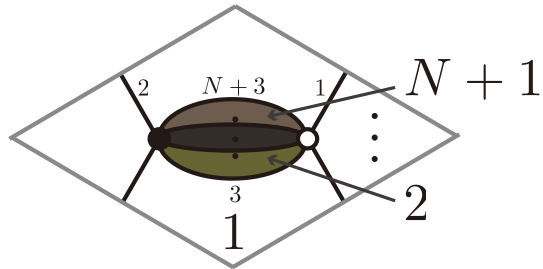


Figure 38: The dimer model for an un-Higgsed \mathbb{C}^3 theory.

multi-bond edge \mathcal{M} in a dimer model. This is a simple extension of the "doubling" procedure, on which we have concentrated in the previous subsections. Let us study the un-Higgsed dimer model which is shown in Fig.38. We shall call the dimer model the one multi-bonded one hexagon model $\mathcal{M}_1\mathcal{H}_1$. The quiver diagram is drawn in Fig.39. This quiver theory has two adjoint chiral fields

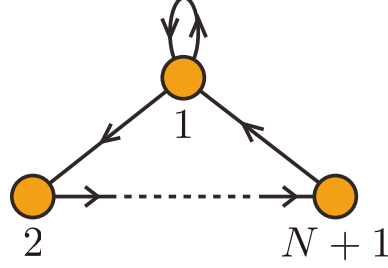


Figure 39: The quiver diagram for an un-Higgsed \mathbb{C}^3 theory. We study the quiver Chern-Simons theory with ${}^t k = (-N, 1, 1, \dots, 1)$.

and $N + 1$ bifundamentals. The superpotential, which has two terms, is given by

$$W = \text{tr}([\Phi_1, \Phi_2] X_{12} X_{23} \cdots X_{N+11}). \quad (5.31)$$

From Fig.38, we can choose perfect matchings as $p_i = \phi_i$. Thus the perfect matching matrix is the unit matrix. Let us consider ${}^t n = (0, 0, 0, 1, 2, \dots, N)$, in other words we discuss the Chern-Simons levels ${}^t k = (-N, 1, 1, \dots, 1)$. Using $n_{m+3} = m$, the Kasteleyn matrix of the quiver Chern-Simons theory is given by

$$K = xp_1 + yp_2 + \sum_{n=1}^N z^{n-1} p_{2+n}. \quad (5.32)$$

Therefore the moduli space of the theory is described by the toric diagram Fig.40. This toric diagram describes the orbifold $\mathbb{C}^2/\mathbb{Z}_N \times \mathbb{C}^2$. Thus we obtain the quiver Chern-Simons theory

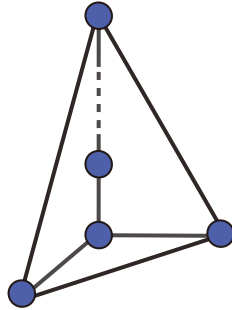


Figure 40: The toric diagram of the moduli space. All the multiplicities of the points are one.

whose moduli space is the orbifold. This theory gives a generalization of the dual ABJM theory: it recover the Phase II by putting $N = 1$.

6 Phases of $C(Q^{111})$ Theory

In this section, we study the phases of the world volume theories of a M2 brane probing the singularity $C(Q^{111})$. This Calabi-Yau singularity is a 4-fold analogue of the conifold $\mathcal{C} = C(T^{11})$. This 4-fold is a homogenous coset space like the conifold:

$$SU(2) \times SU(2) \times SU(2)/U(1) \times U(1). \quad (6.1)$$

An important point is that the M2 brane theories we discuss here are expected to be AdS/CFT dual to the Freund-Rubin $AdS_4 \times Q^{111}$ solution of M-theory vacua. In this paper we focus on the field theory side and we construct three quiver Chern-Simons theories whose moduli space is precisely $C(Q^{111})$. One of these theories is new, and the others have already given in the previous works [54]. The approach using grandparent theories gives an unified perspective for the construction of these theories.

6.1 The $\mathcal{D}_2\mathcal{C}$ model: an un-Higgsing of the conifold grandparent

Let us consider what is a grandparent whose toric diagram is contained in a projection of that of $C(Q^{111})$ as a subdiagram. First we investigate a specific projection shown in Fig.41. We study other types of projection in the latter part of this section. The projected toric diagram in Fig.41

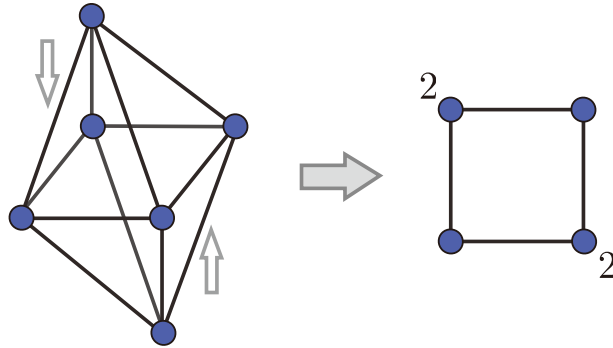


Figure 41: A projection of the toric diagram which gives the conifold as the grandparent theory for $C(Q^{111})$.

is identical with one of the conifold up to multiplicities. Thus the Calabi-Yau 4-fold $C(Q^{111})$ with this projection involves the conifold theory \mathcal{C} as a grandparent theory which generates a phase of the 4-fold.

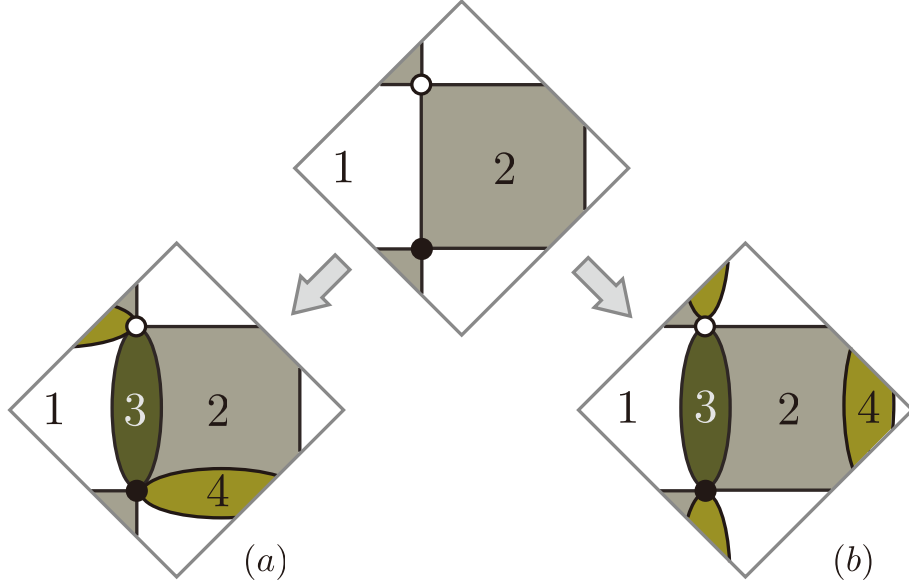


Figure 42: $\mathcal{D}_2\mathcal{C}$ models: Un-Higgsings of the \mathcal{C} dimer model.

Next we have to find an un-Higgsing of the grandparent theory which recovers the 4-fold $C(Q^{111})$ as the moduli space after turning on specific Chern-Simons levels. There exist simple examples of un-Higgsing as Fig.42. The dimer (a) at the left side of the figure implies a phase of D_3 theory, which was shown in [27]. Now we investigate the another dimer (b). The quiver diagram associated with the dimer (b) is indicated in Fig.44. There are 6 matter chiral fields in this theory since the number of edges of the dimer is 6. The superpotential of the theory is

$$W = \epsilon_{st} \text{tr} \left(X_{12}^s X_{23} X_{31} X_{12}^t X_{24} X_{41} \right). \quad (6.2)$$

X_{12}^s 's form a doublet of a global $SU(2)$ symmetry. The incidence matrix of the dimer (b) is given by

$$d = \begin{array}{c|cccc} & 1 & 2 & 3 & 4 \\ \hline X_{13}^1 & 1 & 0 & -1 & 0 \\ X_{13}^2 & 0 & 1 & -1 & 0 \\ X_{34}^1 & 0 & 0 & 1 & -1 \\ X_{34}^2 & 0 & 0 & 1 & -1 \\ X_{41} & -1 & 0 & 0 & 1 \\ X_{42} & 0 & -1 & 0 & 1 \end{array} \quad (6.3)$$

The Kasteleyn matrix of the dimer (b) is 1×1 matrix:

$$\begin{aligned} K &= X_{13}^1 + X_{13}^2 x^{-1} y^{-1} + X_{34}^1 x^{-1} + X_{34}^2 y^{-1} + X_{41} + X_{42} x^{-1} y^{-1} \\ &= p_1 + p_2 x^{-1} y^{-1} + p_3 x^{-1} + p_4 y^{-1} + p_5 + p_6 x^{-1} y^{-1}. \end{aligned} \quad (6.4)$$

This leads to 6 perfect matchings, and we therefore obtain the suitable multiplicities as Fig.43. In the following, these perfect matchings will be uplifted and lowered in order to construct an octahedron as the toric diagram of the moduli space. The structure of the perfect matchings p_α

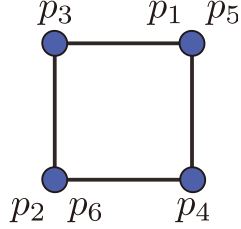


Figure 43: The projected toric diagram of the un-Higgsed theory (b).

are encoded in the diagonal perfect matching matrix:

$$P = \begin{array}{c|cccccc} & p_1 & p_2 & p_3 & p_4 & p_5 & p_6 \\ \hline X_{13}^1 & 1 & 0 & 0 & 0 & 0 & 0 \\ X_{13}^2 & 0 & 1 & 0 & 0 & 0 & 0 \\ X_{34}^1 & 0 & 0 & 1 & 0 & 0 & 0 \\ X_{34}^2 & 0 & 0 & 0 & 1 & 0 & 0 \\ X_{41} & 0 & 0 & 0 & 0 & 1 & 0 \\ X_{42} & 0 & 0 & 0 & 0 & 0 & 1 \end{array} \quad (6.5)$$

There exist 4 choices of uplifting. First we study the condition that the perfect matchings p_2 and p_5 (or p_6 and p_1) are uplifted and lowered and the points form the toric diagram of $C(Q^{111})$. In other words, the perfect matchings p_2 and p_5 obtain nonzero z -coordinates by turning on Chern-Simons levels:

$$q_{p_2} = \pm 1, \quad q_{p_5} = \mp 1, \quad q_\alpha = 0 \text{ otherwise.} \quad (6.6)$$

Using the relation $q = {}^t P \cdot n$, we see that two components of the vector n are nonzero:

$$n_{X_{13}^2} = \pm 1, \quad n_{X_{41}} = \mp 1. \quad (6.7)$$

This choice of n and the incidence matrix (6.3) imply the following choice of Chern-Simons levels:

$${}^t k = \pm(1, 1, -1, -1). \quad (6.8)$$

This theory is one of $C(Q^{111})$ theories which was obtained in [21].

The another theory which was found in [21] corresponds to an another choice of perfect matchings which will be uplifted. Next let us lift up the perfect matchings p_2 and p_1 (or p_6 and p_5) in order that the resulting toric diagram describes the 4-fold of our interest $C(Q^{111})$. In this case, the nonzero components of n are

$$n_{X_{13}^2} = \pm 1, \quad n_{X_{13}^1} = \mp 1 \quad (6.9)$$

and therefore

$${}^t k = \pm(1, -1, 0, 0). \quad (6.10)$$

This is precisely the another choice of the Chern-Simons levels in [21].

Thus we rederive the quiver Chern-Simons theories Fig.44 with the Chern-Simons levels (6.8) and (6.10), which were obtained in [21]. Our derivation is relied on a projection of the toric diagram

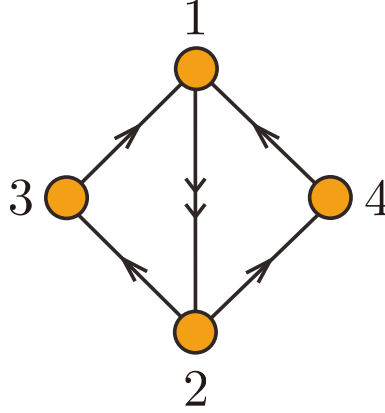


Figure 44: The quiver diagram of the $\mathcal{D}_2\mathcal{C}$ model for $C(Q^{111})$ theory. The Chern-Simons levels are ${}^t k = \pm(1, 1, -1, -1)$ or ${}^t k = \pm(1, -1, 0, 0)$.

and a choice of a grandparent. Thus we can derive other theories for $C(Q^{111})$, since an other choice of a grandparent and an un-Higgsing involves a new theory. In the following, we find other phases of $C(Q^{111})$ theory.

6.2 The \mathcal{S}_4 model: Phase I of $C(\mathbb{F}_0)$ as a grandparent

Let us consider the element of $SL(3, \mathbb{Z})$ transformation

$$M = \begin{pmatrix} 1 & -1 & 0 \\ 1 & 0 & 0 \\ 0 & 0 & 1 \end{pmatrix}. \quad (6.11)$$

It transform the points of the toric diagram of $C(Q^{111})$ as follows:

$$\begin{pmatrix} 0 & 1 & 0 & 0 & 1 & 1 \\ 0 & 0 & 1 & 0 & 1 & 1 \\ 0 & 0 & 0 & 1 & 0 & -1 \end{pmatrix} \rightarrow \begin{pmatrix} 0 & 1 & -1 & 0 & 0 & 0 \\ 0 & 1 & 0 & 0 & 1 & 1 \\ 0 & 0 & 0 & 1 & 0 & -1 \end{pmatrix}. \quad (6.12)$$

Here we collect the points of the toric diagram in the columns of this matrix. The transformation is indicated with the right arrow of Fig.45. In this way, by rotating and projecting the toric diagram

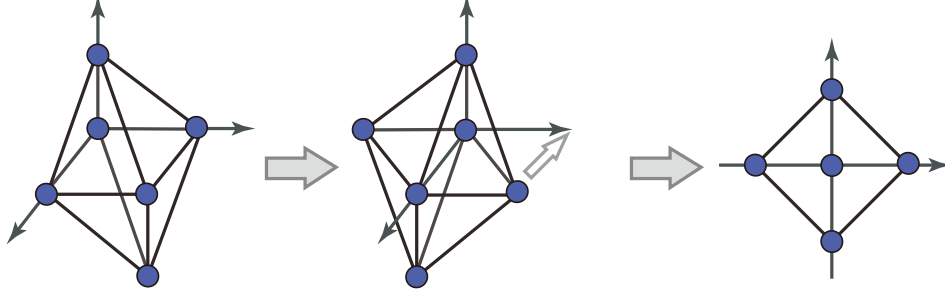


Figure 45: A $SL(3, \mathbb{Z})$ transformation and projection of the toric diagram which give $C(\mathbb{F}_0)$.

of $C(Q^{111})$, we obtain the diagram of $C(\mathbb{F}_0)$ as Fig.45. The \mathbb{F}_0 theory may be therefore able to fill the role of the grandparent theory of $C(Q^{111})$. As we will see in this section, the \mathbb{F}_0 theory actually leads to quiver Chern-Simons theories whose moduli spaces are $C(Q^{111})$.

We begin by studying the phase I of \mathbb{F}_0 [29][30]. Fig.46 is the dimer model of this \mathbb{F}_0^{II} theory. There are 8 matter fields, which correspond to 8 edges of the dimer. The indices s, t and u, v label

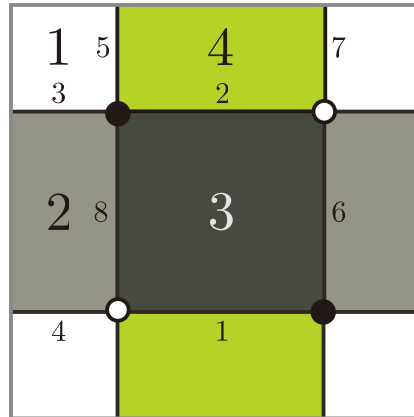


Figure 46: The dimer model for .

the fundamentals of two global $SU(2)$'s. The superpotential is given by

$$W = \epsilon_{st} \epsilon_{uv} \text{tr} (X_{12}^s X_{23}^u X_{34}^t X_{41}^v). \quad (6.13)$$

We can construct the 2×2 Kasteleyn matrix of the grandparent:

$$\begin{aligned} K &= \begin{pmatrix} X_{34}^1 + X_{12}^2 x & X_{23}^1 + X_{41}^2 y^{-1} \\ X_{23}^2 + X_{41}^1 y & X_{34}^2 + X_{12}^1 x^{-1} \end{pmatrix} \\ &= \begin{pmatrix} \phi_1 + \phi_4 x & \phi_6 + \phi_7 y^{-1} \\ \phi_8 + \phi_5 y & \phi_2 + \phi_3 x^{-1} \end{pmatrix}. \end{aligned} \quad (6.14)$$

The permanent of the matrix is given by

$$\begin{aligned} K &= \phi_1 \phi_2 + \phi_3 \phi_4 + x^{-1} \phi_1 \phi_3 + x \phi_2 \phi_4 \\ &\quad + \phi_5 \phi_7 + \phi_6 \phi_8 + y \phi_5 \phi_6 + y^{-1} \phi_7 \phi_8. \end{aligned} \quad (6.15)$$

We thus obtain 8 perfect matchings which form a square toric diagram with an internal point as Fig.47. The monomials of the polynomial give the perfect matching matrix:

$$P = \begin{array}{c|cccccccc} & p_1 & p_2 & q_1 & q_2 & r_1 & r_2 & s_1 & s_2 \\ \hline \phi_1 & 1 & & 1 & & & & & \\ \phi_2 & 1 & & & 1 & & & & \\ \phi_3 & & 1 & 1 & & & & & \\ \phi_4 & & 1 & & 1 & & & & \\ \phi_5 & & & & & 1 & & 1 & \\ \phi_6 & & & & & 1 & & & 1 \\ \phi_7 & & & & & & 1 & 1 & \\ \phi_8 & & & & & & 1 & & 1 \end{array} \quad (6.16)$$

These perfect matchings form the toric diagram of $C(\mathbb{F}_0)$ as Fig.47. There exist many possibilities

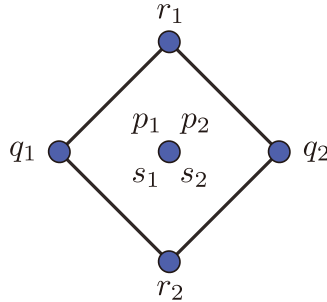


Figure 47: The toric diagram of the \mathbb{F}_0^I grandparent.

for a lift of the toric diagram according to Fig.48. The structure of the perfect matchings (6.16) involves the following two cases.

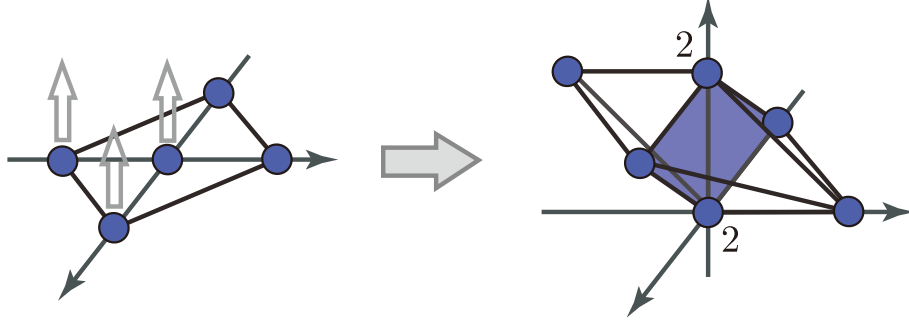


Figure 48: The uplift of the toric diagram. Two points have the multiplicity 2.

(i) lift of p_1, s_1 (or p_2, s_2), q_2 and r_2

First we consider the case where the points p_1, s_1, q_2 and r_2 are uplifted. In this case, we have to choose n in order that the third coordinates of the lifted toric diagram are

$${}^tq = (1, 0, 0, 1, 0, 1, 1, 0). \quad (6.17)$$

Using the relation $q = {}^tP \cdot n$, we find that the vector n must satisfy the following equations:

$$\begin{aligned} n_1 + n_2 &= 1, & n_1 + n_3 &= 0, & n_3 + n_4 &= 0, & n_2 + n_4 &= 1 \\ n_5 + n_6 &= 0, & n_5 + n_7 &= 1, & n_7 + n_8 &= 1, & n_6 + n_8 &= 0. \end{aligned}$$

These constraints have the following integral solutions for $l, m \in \mathbb{Z}$:

$${}^tn = (l, 1 - l, -l, l, m, -m, 1 - m, m). \quad (6.18)$$

Recall the incidence matrix for the dimer Fig.46:

$$d = \begin{array}{c|cccccccc} & p_1 & p_2 & q_1 & q_2 & r_1 & r_2 & s_1 & s_2 \\ \hline 1 & & & 1 & 1 & -1 & & -1 & \\ 2 & & & -1 & -1 & & 1 & & 1 \\ 3 & 1 & 1 & & & & -1 & & -1 \\ 4 & -1 & -1 & & & 1 & & 1 & \end{array} \quad (6.19)$$

Then these choices of the vector n give the unique Chern-Simons level vector:

$${}^tk = (-1, 0, 1, 0). \quad (6.20)$$

The point here is that the Chern-Simons levels are independent of the choice of the integers l and m .

(ii) lift of p_1, s_2 (or p_2, s_1), q_2 and r_2

Next let us study the case where the third coordinate of the lifted toric diagram is given by

$${}^tq = (1, 0, 0, 1, 0, 1, 0, 1). \quad (6.21)$$

We realize this uplift by imposing the following constraints for n .

$$\begin{aligned} n_1 + n_2 &= 1, & n_1 + n_3 &= 0, & n_3 + n_4 &= 0, & n_2 + n_4 &= 1 \\ n_5 + n_6 &= 0, & n_5 + n_7 &= 0, & n_7 + n_8 &= 1, & n_6 + n_8 &= 1. \end{aligned}$$

They have the following integral solutions for $l, m \in \mathbb{Z}$:

$${}^tn = (l, 1 - l, -l, l, m, -m, -m, 1 + m). \quad (6.22)$$

These choices of the vector n lead to the unique Chern-Simons level vector:

$${}^tk = (0, 1, 0, -1). \quad (6.23)$$

The Chern-Simons levels are also independent of the choice of the integers l and m .

We thus obtain the quiver Chern-Simons theories for $C(Q^{111})$ as is shown in Fig.49. These theories have been constructed in [34]. Our prescription gives the new derivation of the Aganagic theory by the argument of toric geometry of the moduli space. Notice that the moduli space become

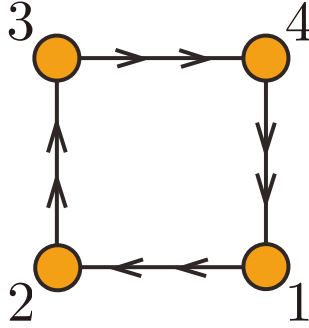


Figure 49: The quiver diagram of the $C(Q^{111})$ theory. The Chern-Simons levels are ${}^tk = \pm(1, 0, -1, 0)$ or $\pm(0, 1, 0, -1)$.

the orbifold $C(Q^{111})/\mathbb{Z}_2$, as was shown in [26], if we choose the Chern-Simons levels as follows:

$${}^tk = (1, 1, -1, -1). \quad (6.24)$$

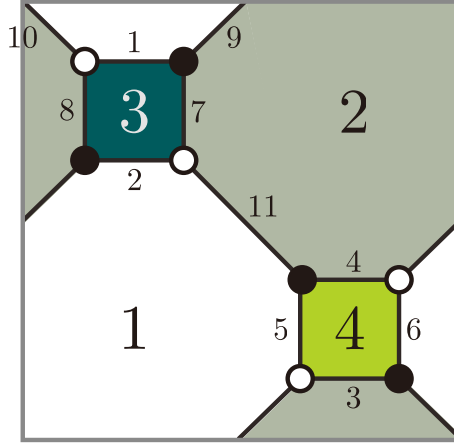


Figure 50: The dimer model for the \mathbb{F}_0^{II} theory.

6.3 The $\mathcal{S}_2\mathcal{O}_2$ model: Phase II of $C(\mathbb{F}_0)$ as a grandparent

At the end of this section, we extend the above arguments for Phase II of the \mathbb{F}_0 theory [29][30]. The dimer model of the Phase II \mathbb{F}_0^{II} theory is shown in Fig.50. This theory is called the $\mathcal{S}_2\mathcal{O}_2$ model since this fundamental domain consists of two squares and two octagons. The superpotential is given by

$$W = \epsilon_{st}\epsilon_{uv} \text{tr} \left(X_{12}^{su} X_{23}^v X_{31}^t \right) - \epsilon_{st}\epsilon_{uv} \text{tr} \left(X_{12}^{us} X_{24}^v X_{41}^t \right). \quad (6.25)$$

The quiver encoded in the dimer is drawn in Fig.52.

Let us study the \mathbb{F}_0^{II} theory with the Kasteleyn matrix analysis. The Kasteleyn matrix of Fig.50 is given by

$$K = \begin{pmatrix} \phi_8 & \phi_1 & 0 & x^{-1}y^{-1}\phi_{10} \\ \phi_2 & \phi_7 & \phi_{11} & 0 \\ 0 & x\phi_{12} & \phi_5 & \phi_3 \\ y\phi_9 & 0 & \phi_4 & \phi_6 \end{pmatrix}. \quad (6.26)$$

The permanent of the matrix is the following 12×9 matrix:

$$\begin{aligned} \text{perm}K &= \phi_1\phi_2\phi_5\phi_6 + \phi_3\phi_4\phi_7\phi_8 + \phi_1\phi_2\phi_3\phi_4 + \phi_5\phi_6\phi_7\phi_8 + \phi_9\phi_{10}\phi_{11}\phi_{12} \\ &+ x\phi_6\phi_8\phi_{11}\phi_{12} + x^{-1}\phi_5\phi_7\phi_9\phi_{10} + y\phi_1\phi_3\phi_9\phi_{11} + y^{-1}\phi_2\phi_4\phi_{10}\phi_{12}. \end{aligned} \quad (6.27)$$

We find therefore 9 perfect matchings for the \mathbb{F}_0^{II} theory. Recall that the number of perfect matchings for the \mathbb{F}_0^{I} theory is 8. The additional perfect matching corresponds to the internal point at the origin of the 2 dimensional toric diagram. Thus the multiplicity of the internal point is 5 for the \mathbb{F}_0^{I} theory.

The structure of the perfect matchings is also different from these of the \mathbb{F}_0^I theory and therefore we can construct $C(Q^{111})$ theory with different way. We can see the difference by computing the perfect matching matrix. The perfect matching matrix is given by

$$P = \begin{array}{c|cccccccccc} & p_1 & p_2 & q_1 & q_2 & r_1 & r_2 & s_1 & s_2 & s_3 \\ \hline \phi_1 & 1 & & & & 1 & & 1 & & \\ \phi_2 & 1 & & & & & 1 & 1 & & \\ \phi_3 & & 1 & & & 1 & & 1 & & \\ \phi_4 & & 1 & & & & 1 & 1 & & \\ \phi_5 & 1 & & 1 & & & & & 1 & \\ \phi_6 & 1 & & & 1 & & & & 1 & \\ \phi_7 & & 1 & 1 & & & & & 1 & \\ \phi_8 & & 1 & & 1 & & & & 1 & \\ \phi_9 & & & 1 & & 1 & & & & 1 \\ \phi_{10} & & & 1 & & & 1 & & & 1 \\ \phi_{11} & & & & 1 & 1 & & & & 1 \\ \phi_{12} & & & & 1 & & 1 & & & 1 \end{array} \quad (6.28)$$

In order to obtain the octahedron toric diagram of $C(Q^{111})$ as the moduli space of the resulting Chern-Simons theory, we have to uplift q_1 , r_2 , and some internal points for instance. First let us turn on n_{10} for this purpose, and 3 points thereby get nonzero third coordinates:

$$q_\alpha = 1 \text{ for } \alpha = q_1, r_2, s_3. \quad (6.29)$$

This uplift is drawn in Fig.51. In this way we obtain an octahedron which describes the toric data of $C(Q^{111})$. This choice of n corresponds to the following Chern-Simons levels:

$${}^t k = (1, -1, 0, 0). \quad (6.30)$$

We can also obtain the same moduli space by turning on n_2 and n_7 . We choose n as

$$n_2 = n_7 = 1, \quad n_i = 0 \text{ otherwise}, \quad (6.31)$$

thereby lifting six points along the direction of the z-axis. The nonzero z-coordinates are given by

$$q_\alpha = 1 \text{ for } \alpha = q_1, r_2, p_1, p_2, s_1, s_2. \quad (6.32)$$

In this way we obtain an octahedron diagram which is $SL(3, \mathbb{Z})$ equivalent to the previous one. The Chern-Simons levels associated with the choice of n are

$${}^t k = (-1, 1, 0, 0). \quad (6.33)$$

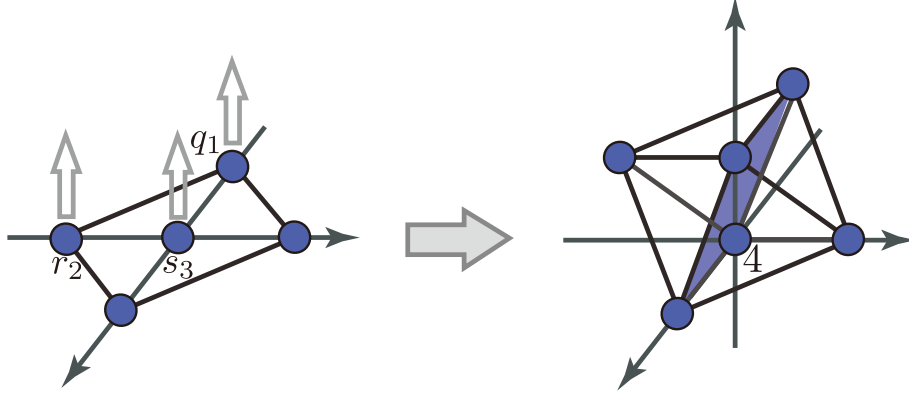


Figure 51: The uplift of the toric diagram. One of the multiplicities of the resulting toric diagram is 4.

Thus we get the $\mathcal{N} = 2$ quiver Chern-Simons theory whose moduli space is the Calabi-Yau cone of the Sasaki-Einstein manifold Q^{111} . The quiver diagram and the Chern-Simons levels are shown in Fig.52. We propose that this theory describes a new phase of the Q^{111} theory which is a toic

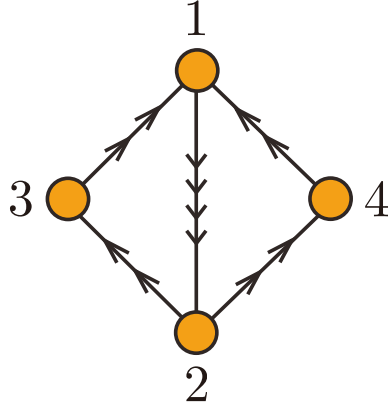


Figure 52: The quiver diagram of the Q^{111} theory with the $\mathcal{S}_2\mathcal{O}_2$ dimer model. The Chern-Simons levels are ${}^t k = (1, -1, 0, 0)$ or $(-1, 1, 0, 0)$.

dual of the previous two phases.

7 Conclusion

In this article we study $\mathcal{N} = 2$ quiver Chern-Simons theories whose moduli spaces are toric Calabi-Yau 4-fold. We discuss the relation between Aganagic's stringy derivation of M2 brane theories and the forward algorithm of quiver Chern-Simons theories, and we observe that the forward algorithm

implies the set-up of Aganagic if the Chern-Simons theory has a consistent parent theory in $3 + 1$ dimensions. Meanwhile we see that Chern-Simons theories without superconformal parent theory give fractional GLSM $U(1)$ charge, which might be a sign of inconsistency. It would be of interest to give stringy understanding of this property.

We also construct quiver Chern-Simons theories which do not have a superconformal parent but have a Calabi-Yau moduli spaces. In order to construct a quiver Chern-Simons theory associated with a specific toric 4-fold, 2-dimensional diagram obtained by projection the toric diagram onto plane is important. These projected toric diagram, in general, can not be realized as the moduli space of a $3 + 1$ dimensional quiver theory, and thus we can not find parent theory for generic situation. We find that the grandparent theory that emerges from the projected toric diagram is a useful starting point. The moduli space of this grandparent has the toric diagram which is a sub-diagram of the projected one. By un-Higgsing the grandparent theory, i.e. by adding points to the toric diagram, we can construct the quiver theory whose toric diagram is the same as the projected one. Then we can recover the 3 dimensional toric diagram by turning on an appropriate Chern-Simons levels. Using this scheme, we give many quiver Chern-Simons theories: M2 brane theory for $\mathbb{C}^2/\mathbb{Z}_2 \times \mathbb{C}^2$, $C(dP_3) \times \mathbb{C}$ and $C(Q^{111})$ for instance. The grandparent theory gives a unified perspective for the derivation of toric phases of these theories.

Understanding the stringy meaning of quiver Chern-Simons theories without parent theory is an important issue. Dualities, such as mirror symmetry[47], might play a key role to derive these theory from string theory set-up. It is also important to study AdS/CFT duality for our M2 brane theories. Since $C(Q^{111})$, for instance, has a well-studied gravity dual, we might judge the right or wrong of our proposal. We expect that these approach from string theory would give hint to understand the observation that there exist many toric phases for M2 brane theories, especially theories without consistent parents. We leave these for future work.

Acknowledgements

M.T. is supported by JSPS Grant-in-Aid for Creative Scientific Research, No.19GS0219.

Appendix

A The cofactor expansion of permanents

The permanent of a matrix K is, roughly speaking, a modification of the determinant, which is a sum over permutations without weighting by sign. The definition is given by

$$\text{perm}K = \sum_{\sigma \in S_N} K_{1\sigma(1)} K_{2\sigma(2)} \cdots K_{N\sigma(N)}. \quad (\text{A.1})$$

It is easy to prove that we can expand the permanent using the cofactor:

$$\begin{aligned} \text{perm}K &= \sum_{n=1}^N K_{1N} \sum_{\tilde{\sigma} \in S_N | \tilde{\sigma}(1)=n} K_{2\tilde{\sigma}(2)} \cdots K_{N\tilde{\sigma}(N)} \\ &= \sum_{n=1}^N K_{1N} \text{perm}\tilde{K}_n. \end{aligned} \quad (\text{A.2})$$

Here \tilde{K}_n is the cofactor of K with respect to the 1-th row and n -th column.

By using the cofactor expansion (A.2), we can compute the permanent of various Kasteleyn matrices. In this appendix, we show the equation (5.9). The application of the cofactor expansion (A.2) to the Kasteleyn matrix (5.8) implies the following relation:

$$\begin{aligned} \text{perm}K(a, b, c; x, y) &\equiv \text{perm} \begin{pmatrix} a_1 + b_1x & 0 & \cdots & 0 & 0 & c_N y \\ c_1 & a_2 + b_2x & & 0 & 0 & 0 \\ & & \dots\dots\dots & & & \\ 0 & 0 & & a_{N-2} + b_{N-2} & 0 & 0 \\ 0 & 0 & & c_{N-2} & a_{N-1} + b_{N-1}x & 0 \\ 0 & 0 & \cdots & 0 & c_{N-1} & a_N + b_N x \end{pmatrix} \\ &= y c_N \text{perm} \begin{pmatrix} c_1 & a_2 + b_2x & & 0 & 0 \\ & & \dots\dots & & \\ 0 & 0 & & a_{N-2} + b_{N-2} & 0 \\ 0 & 0 & & c_{N-2} & a_{N-1} + b_{N-1}x \\ 0 & 0 & \cdots & 0 & c_{N-1} \end{pmatrix} \\ &\quad + (a_N + x b_N) \text{perm} \begin{pmatrix} a_1 + b_1x & 0 & \cdots & 0 & 0 \\ c_1 & a_2 + b_2x & & 0 & 0 \\ & & \dots\dots & & \\ 0 & 0 & & a_{N-2} + b_{N-2} & 0 \\ 0 & 0 & \cdots & c_{N-2} & a_{N-1} + b_{N-1}x \end{pmatrix}. \end{aligned}$$

Meanwhile we can compute the permanent of the following matrix by using the cofactor expansion:

$$\text{perm} \begin{pmatrix} X_1 & Y_1 & \dots & 0 & 0 \\ 0 & X_2 & Y_2 & 0 & 0 \\ & & \dots & & \\ 0 & 0 & \dots & X_{N-1} & Y_{N-1} \\ 0 & 0 & \dots & 0 & X_N \end{pmatrix} = \prod_n X_n. \quad (\text{A.3})$$

By applying this formula to $\text{perm}K(a, b, c; x, y)$, we find

$$\text{perm}K(a, b, c; x, y) = y \prod_n c_n + \prod_n (a_n + x b_n). \quad (\text{A.4})$$

References

- [1] J. H. Schwarz, “Superconformal Chern-Simons theories,” JHEP **0411**, 078 (2004) [arXiv:hep-th/0411077].
- [2] J. Bagger and N. Lambert, “Gauge Symmetry and Supersymmetry of Multiple M2-Branes,” Phys. Rev. D **77**, 065008 (2008) [arXiv:0711.0955 [hep-th]].
- [3] J. Bagger and N. Lambert, “Comments On Multiple M2-branes,” JHEP **0802**, 105 (2008) [arXiv:0712.3738 [hep-th]].
- [4] A. Gustavsson, “Algebraic structures on parallel M2-branes,” Nucl. Phys. B **811**, 66 (2009) [arXiv:0709.1260 [hep-th]].
- [5] M. Van Raamsdonk, “Comments on the Bagger-Lambert theory and multiple M2-branes,” JHEP **0805**, 105 (2008) [arXiv:0803.3803 [hep-th]].
- [6] D. Gaiotto and E. Witten, “Janus Configurations, Chern-Simons Couplings, And The Theta-Angle in N=4 Super Yang-Mills Theory,” arXiv:0804.2907 [hep-th].
- [7] K. Hosomichi, K. M. Lee, S. Lee, S. Lee and J. Park, “N=4 Superconformal Chern-Simons Theories with Hyper and Twisted Hyper Multiplets,” JHEP **0807**, 091 (2008) [arXiv:0805.3662 [hep-th]].
- [8] D. Gaiotto and X. Yin, “Notes on superconformal Chern-Simons-matter theories,” JHEP **0708**, 056 (2007) [arXiv:0704.3740 [hep-th]].
- [9] K. Hosomichi, K. M. Lee, S. Lee, S. Lee and J. Park, “N=5,6 Superconformal Chern-Simons Theories and M2-branes on Orbifolds,” JHEP **0809**, 002 (2008) [arXiv:0806.4977 [hep-th]].

- [10] N. Lambert and D. Tong, “Membranes on an Orbifold,” *Phys. Rev. Lett.* **101**, 041602 (2008) [arXiv:0804.1114 [hep-th]].
- [11] J. Distler, S. Mukhi, C. Papageorgakis and M. Van Raamsdonk, “M2-branes on M-folds,” *JHEP* **0805**, 038 (2008) [arXiv:0804.1256 [hep-th]].
- [12] O. Aharony, O. Bergman, D. L. Jafferis and J. Maldacena, “N=6 superconformal Chern-Simons-matter theories, M2-branes and their gravity duals,” *JHEP* **0810**, 091 (2008) [arXiv:0806.1218 [hep-th]].
- [13] M. Benna, I. Klebanov, T. Klose and M. Smedback, “Superconformal Chern-Simons Theories and AdS_4/CFT_3 Correspondence,” *JHEP* **0809**, 072 (2008) [arXiv:0806.1519 [hep-th]].
- [14] D. Martelli and J. Sparks, “Moduli spaces of Chern-Simons quiver gauge theories and $AdS(4)/CFT(3)$,” *Phys. Rev. D* **78**, 126005 (2008) [arXiv:0808.0912 [hep-th]].
- [15] K. Ueda and M. Yamazaki, “Toric Calabi-Yau four-folds dual to Chern-Simons-matter theories,” *JHEP* **0812**, 045 (2008) [arXiv:0808.3768 [hep-th]].
- [16] A. Hanany and A. Zaffaroni, “Tilings, Chern-Simons Theories and M2 Branes,” *JHEP* **0810**, 111 (2008) [arXiv:0808.1244 [hep-th]].
- [17] A. Hanany and K. D. Kennaway, “Dimer models and toric diagrams,” arXiv:hep-th/0503149.
- [18] S. Franco, A. Hanany, K. D. Kennaway, D. Vegh and B. Wecht, “Brane Dimers and Quiver Gauge Theories,” *JHEP* **0601**, 096 (2006) [arXiv:hep-th/0504110].
- [19] S. Franco, A. Hanany, D. Martelli, J. Sparks, D. Vegh and B. Wecht, “Gauge theories from toric geometry and brane tilings,” *JHEP* **0601**, 128 (2006) [arXiv:hep-th/0505211].
- [20] A. Hanany, D. Vegh and A. Zaffaroni, “Brane Tilings and M2 Branes,” *JHEP* **0903**, 012 (2009) [arXiv:0809.1440 [hep-th]].
- [21] S. Franco, A. Hanany, J. Park and D. Rodriguez-Gomez, “Towards M2-brane Theories for Generic Toric Singularities,” *JHEP* **0812**, 110 (2008) [arXiv:0809.3237 [hep-th]].
- [22] S. Lee, “Superconformal field theories from crystal lattices,” *Phys. Rev. D* **75**, 101901 (2007) [arXiv:hep-th/0610204].
- [23] S. Lee, S. Lee and J. Park, “Toric $AdS(4)/CFT(3)$ duals and M-theory crystals,” *JHEP* **0705**, 004 (2007) [arXiv:hep-th/0702120].

- [24] S. Kim, S. Lee, S. Lee and J. Park, “Abelian Gauge Theory on M2-brane and Toric Duality,” Nucl. Phys. B **797**, 340 (2008) [arXiv:0705.3540 [hep-th]].
- [25] Y. Imamura and K. Kimura, “Quiver Chern-Simons theories and crystals,” JHEP **0810**, 114 (2008) [arXiv:0808.4155 [hep-th]].
- [26] S. Franco, I. R. Klebanov and D. Rodriguez-Gomez, “M2-branes on Orbifolds of the Cone over $Q^{1,1,1}$,” JHEP **0908**, 033 (2009) [arXiv:0903.3231 [hep-th]].
- [27] J. Davey, A. Hanany, N. Mekareeya and G. Torri, “Phases of M2-brane Theories,” JHEP **0906**, 025 (2009) [arXiv:0903.3234 [hep-th]].
- [28] J. Davey, A. Hanany, N. Mekareeya and G. Torri, “Higgsing M2-brane Theories,” arXiv:0908.4033 [hep-th].
- [29] B. Feng, A. Hanany and Y. H. He, “D-brane gauge theories from toric singularities and toric duality,” Nucl. Phys. B **595**, 165 (2001) [arXiv:hep-th/0003085].
- [30] B. Feng, A. Hanany and Y. H. He, “Phase structure of D-brane gauge theories and toric duality,” JHEP **0108**, 040 (2001) [arXiv:hep-th/0104259].
- [31] C. E. Beasley and M. R. Plesser, “Toric duality is Seiberg duality,” JHEP **0112**, 001 (2001) [arXiv:hep-th/0109053].
- [32] B. Feng, A. Hanany, Y. H. He and A. M. Uranga, “Toric duality as Seiberg duality and brane diamonds,” JHEP **0112**, 035 (2001) [arXiv:hep-th/0109063].
- [33] B. Feng, S. Franco, A. Hanany and Y. H. He, “Symmetries of toric duality,” JHEP **0212**, 076 (2002) [arXiv:hep-th/0205144].
- [34] M. Aganagic, “A Stringy Origin of M2 Brane Chern-Simons Theories,” arXiv:0905.3415 [hep-th].
- [35] J. Davey, A. Hanany and J. Pasukonis, “On the Classification of Brane Tilings,” arXiv:0909.2868 [hep-th].
- [36] N. Benishti, Y. H. He and J. Sparks, “(Un)Higgsing the M2-brane,” arXiv:0909.4557 [hep-th].
- [37] B. S. Acharya, J. M. Figueroa-O’Farrill, C. M. Hull and B. J. Spence, “Branes at conical singularities and holography,” Adv. Theor. Math. Phys. **2**, 1249 (1999) [arXiv:hep-th/9808014].
- [38] D. R. Morrison and M. R. Plesser, “Non-spherical horizons. I,” Adv. Theor. Math. Phys. **3**, 1 (1999) [arXiv:hep-th/9810201].

- [39] C. Beasley, B. R. Greene, C. I. Lazaroiu and M. R. Plesser, “D3-branes on partial resolutions of abelian quotient singularities of Calabi-Yau threefolds,” Nucl. Phys. B **566**, 599 (2000) [arXiv:hep-th/9907186].
- [40] S. Franco and D. Vegh, “Moduli spaces of gauge theories from dimer models: Proof of the correspondence,” JHEP **0611**, 054 (2006) [arXiv:hep-th/0601063].
- [41] A. Hanany and Y. H. He, “M2-Branes and Quiver Chern-Simons: A Taxonomic Study,” arXiv:0811.4044 [hep-th].
- [42] A. Hanany and Y. H. He, “Chern-Simons: Fano and Calabi-Yau,” arXiv:0904.1847 [hep-th].
- [43] J. Hewlett and Y. H. He, “Probing the Space of Toric Quiver Theories,” arXiv:0909.2879 [hep-th].
- [44] D. Forcella, A. Hanany, Y. H. He and A. Zaffaroni, “The Master Space of N=1 Gauge Theories,” JHEP **0808**, 012 (2008) [arXiv:0801.1585 [hep-th]].
- [45] A. Hanany and D. Vegh, “Quivers, tilings, branes and rhombi,” JHEP **0710**, 029 (2007) [arXiv:hep-th/0511063].
- [46] D. R. Gulotta, “Properly ordered dimers, R -charges, and an efficient inverse algorithm,” JHEP **0810**, 014 (2008) [arXiv:0807.3012 [hep-th]].
- [47] B. Feng, Y. H. He, K. D. Kennaway and C. Vafa, “Dimer models from mirror symmetry and quivering amoebae,” Adv. Theor. Math. Phys. **12**, 3 (2008) [arXiv:hep-th/0511287].
- [48] K. Maruyoshi, M. Taki, S. Terashima and F. Yagi, “New Seiberg Dualities from N=2 Dualities,” JHEP **0909**, 086 (2009) [arXiv:0907.2625 [hep-th]].
- [49] B. Feng, S. Franco, A. Hanany and Y. H. He, “Unhiggsing the del Pezzo,” JHEP **0308**, 058 (2003) [arXiv:hep-th/0209228].
- [50] I. R. Klebanov and E. Witten, “Superconformal field theory on threebranes at a Calabi-Yau singularity,” Nucl. Phys. B **536**, 199 (1998) [arXiv:hep-th/9807080].
- [51] Y. Imamura and K. Kimura, “On the moduli space of elliptic Maxwell-Chern-Simons theories,” Prog. Theor. Phys. **120**, 509 (2008) [arXiv:0806.3727 [hep-th]].
- [52] S. Terashima and F. Yagi, “Orbifolding the Membrane Action,” JHEP **0812**, 041 (2008) [arXiv:0807.0368 [hep-th]].

- [53] Y. Imamura and K. Kimura, “N=4 Chern-Simons theories with auxiliary vector multiplets,” JHEP **0810**, 040 (2008) [arXiv:0807.2144 [hep-th]].
- [54] B. E. W. Nilsson and C. N. Pope, “Hopf Fibration Of Eleven-Dimensional Supergravity,” Class. Quant. Grav. **1**, 499 (1984).